IPPJ-AM-13

ATOMIC PROCESSES IN FUSION PLASMAS

PROCEEDINGS OF THE NAGOYA SEMINAR
ON
ATOMIC PROCESSES IN FUSION PLASMAS

INSTITUTE OF PLASMA PHYSICS
NAGOYA UNIVERSITY

NAGOYA, JAPAN

IPPJ–AM–13

ATOMIC PROCESSES IN FUSION PLASMAS

Proceedings of the Nagoya Seminar
on
Atomic Processes in Fusion Plasmas

Edited by
Yukikazu Itikawa and Takako Kato

Institute of Plasma Physics, Nagoya University
Chikusa-ku, Nagoya 464, Japan

September 5–7, 1979

CONTENTS

PREFACE

Nagoya seminar on Atomic Processes in Fusion Plasmas took place, as a satellite meeting of the Eleventh International Conference on the Physics of Electronic and Atomic Collisions, on 5 - 7 September 1979 at the Institute of Plasma Physics, Nagoya University, Nagoya, Japan. On the 5th of September, the participants visited, on the way from Kyoto to Nagoya, the Pearl Island, Ise Shrine and a famous sukiyaki restaurant. Hot discussions on atomic processes started on the train and buses on the way. A formal presentation of papers was made on the next two days.

The seminar was intended to bring together both atomic and plasma physicists to review and discuss various atomic processes taking part in high-temperature plasmas. There were 81 participants from 13 countries, among whom 38 were from abroad. The Seminar was opened by the address by Professor K. Takayama, Director of the Institute of Plasma Physics, and closed by the concluding remarks by Professor J. Kistemaker, Director of FOM, the Netherlands.

The Proceedings include 8 review papers presented at the Seminar. In addition 19 contributed papers were presented, but they were encouraged to be published in regular journals rather than being included in the Proceedings. The titles of the contributed papers are given in the program reproduced at the end of the Proceedings.

Since the Seminar was one of the rare occassions for both atomic and plasma physicists to meet each other, the list of participants is attached for future communication among each other, so that a mutual exchange between the two fields of research will be still closer.

On behalf of the organizing committee, I would like to express our sincerest thanks to all participants who gave active contribution not only by the formal presentation of papers but also through informal discussions in all possible occasions. I would also mention the achievement of devoted secretariat, Drs. Y. Itikawa, T. Kato and S. Ohtani and also Mrs. K. Kimura and the constructive advices of Professors Y. Kaneko and H. Suzuki.

I acknowledge the financial support of the Japan Society for the Promotion of Science and the contributions of the Chubu Electric Power Co., Inc., Tokai Bank Ltd., Daido Steel Co., Ltd., NGK Insulators Ltd., and Nagoya Rail Road Co., Ltd.

Satio Hayakawa
Chairman
Organizing Committee
of the Nagoya Seminar

Organizing Committee

J. Fujita (Inst. Plasma Phys.)
K. Fukuda (Kyoto Univ.)
S. Hayakawa, Chairman (Inst. Plasma Phys.)
Y.H. Ichikawa (Inst. Plasma Phys.)
Y. Itikawa, Secretary (Inst. Plasma Phys.)
T. Iwai (Osaka Univ.)
Y. Kaneko (Tokyo Metropolitan Univ.)
T. Kato (Inst. Plasma Phys.)
A. Miyahara (Inst. Plasma Phys.)
S. Ohtani, Secretary (Inst. Plasma Phys.)
M. Otsuka (Inst. Plama Phys.)
H. Suzuki (Sophia Univ.)
K. Takayama (Inst. Plasma Phys.)

Local Committee

T. Fujimoto (Kyoto Univ.)
J. Fujita (Inst. Plasma Phys.)
S. Hayakawa (Inst. Plasma Phys.)
Y. Itikawa (Inst. Plasma Phys.)
T. Iwai (Osaka Univ.)
Y. Kaneko (Tokyo Metropolitan Univ.)
T. Kato (Inst. Plasma Phys.)
S. Ohtani (Inst. Plasma Phys.)
H. Suzuki (Sophia Univ.)
S. Watanabe (Mie Univ.)

The Nagoya Seminar is partly supported by the Japan Society for the Promotion of Science.

ATOMIC PROCESSES IN PLASMAS

Satio Hayakawa

Department of Astrophysics and Institute of Plasma Physics
Nagoya University, Nagoya 464, Japan

INTRODUCTION

Since the early history of controlled nuclear fusion study, it has been generally recongnized that the energy gain by thermonuclear reactions should exceed the energy loss by radiation and particles. The loss rate was evaluated for thermal bremsstrahlung from a fully ionized plasma and for diffusion across a magnetic field. In practice, however, impurities mixed with injected fuel gas and fed by wall materials take part in various loss processes.

Since heavy impurity elements are partially ionized, line emission therefrom gives a major contribution to the radiation loss, as is well known for hot celestial plasmas, even if the relative density of impurities is very small. The temperature dependence of radiation rate has a negative slope in some temperature ranges, and this gives rise to thermal instabilities. The collision of fuel ions with partially ionized ions results in the loss of hot particles by charge exchange. All these effects enhance the energy loss rate.

On the other hand, the presence of impurities serves for plasma diagnostics. The intensities and profiles of emission lines give us information on plasma parameters such as the density and temperature. In interpreting experimental results, however, one has to keep in mind that the ionization equilibrium rarely holds. In some cases, the thermal equilibrium between electrons and ions does not hold. Under these non-equilibrium conditions, the energy loss rate is considerably different from that under equilibrium.

A radical modification of atomic processes is necessary for a very dense plasma, such as the one coming into play in the inertial confinement fusion. Because of a high rate of collisions, only a few bound levels are left, and the rest would merge with continuum.

In the present review I shall discuss these problems which have thus far not deeply been considered. Because of time limitation, I shall concentrate myself to electron-ion collisions which are relevant to radiation processes.

RADIATION FROM THIN PLASMA UNDER IONIZATION EQUILIBRIUM

The relative abundances of ions are determined by the balance between ionization and recombination. The rate of ionization increases rapidly with electron temperature T, whereas the recombination rate decreases slowly as T increases. The rapid increase of the former is mainly dictated by a factor exp (-I/T) where I is the ionization energy. In the first approximation, therefore, the balance between two processes is attained for a given value of I/T. In the next approximation, however, factors depending separately on I and T give appreciable contributions. As a result, the temperature for the maximum abundance of an ion species is roughly proportional to I^k, where k is somewhat larger than unity.

The temperature at which the radiation loss rate is maximum, T_m, is slightly higher than that for the maximum ion abundance, because a rapid increase of the collisional exciation rate with temperature. The radiation loss rate is proportional to $T^{-1/2} \exp(-E_x/T)$, where E_x is the excitation energy. Since $E_x \propto I$ and T_m and I are related to one another as discussed above, the radiation loss rate near the maximum ion abundance depends very weakly on the atomic number for a given shell.

A numerical calculation by Kato [1,2] demonstrates the above feature, as shown in Figure 1. An approximate relation

$$T_m \propto Z^p \tag{1}$$

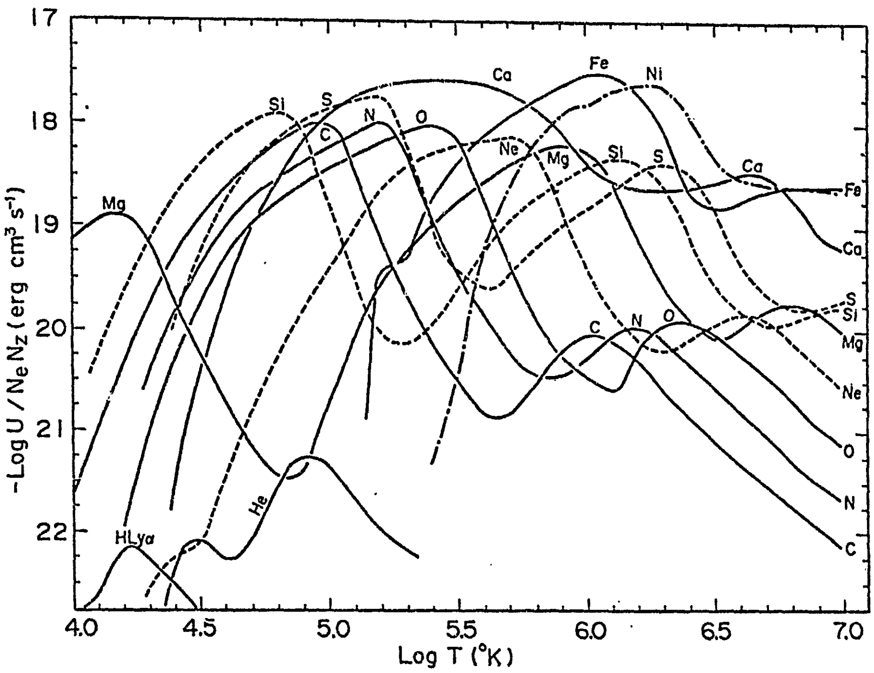

Fig.1. The rates of energy loss, U, by line emission, divided by the atomic density N_Z and the electron density N_e, versus electron temperature T. Ion abundances under ionization equilibrium are assumed.

holds with p = 2.5, 3.3 and 4.0 for the K-, L-, and M-shells, respectively. A numerical calculation with a simplified model by Post et al[3] also gives a similar result.

If the radiation loss rate is compared with that by thermal bremsstrahlung of a hydrogen plasma, the latter is dominated by the line emission from impurity ions for the contamination of K-shell ions greater than 10^{-3} and for that of outer shell ions greater than 10^{-5}. This gives a rough idea how important is the contribution of impurities to the radiation energy loss.

For $T > T_m$ the radiation loss rate decreases, until the excitation of lines of an inner shell becomes effective. The negative slope against T implies that thermal instabilities may arise in such a temperature range. In the boundary region of a hot plasma the temperature gradient is large, and the disruption of a plasma may well take place due to thermal instabilities.

NON-EQUILIBRIUM STATES

If a plasma phenomenon occurs in a time scale shorter than the time scales of atomic processes, the plasma does not reach an equilibrium state. Depending on the mode of heating, the energy fed into a plasma is first transferred to electrons or ions. Hence the electron temperature, which is directly relevant to line emission, is higher or lower than the average temperature during the time shorter than the electron-ion relaxation time. This fact should be kept in mind in the analysis of spectroscopic data.

Even after the electron-ion equilibrium is attained, ion abundances may be far from equilibrium values. Since the ionization rate is generally greater than the recombination rate, the degree of ionization increases with time after the electron temperature is raised, and then gradually decreases to approach the equilibrium value. If the plasma is cooled, recombination proceeds slowly.

In the former case the plasma is in an ionizing stage, and the distribution of ion abundances is shifted to a lower degree of ionization in the early phase and to a higher degree in the later phase in comparison with that in ionization equilibrium. In the latter case the plasma is in a recombining stage, and the degree of ionization is left higher than that in ionization equilibrium.

We shall illustrate in Figure 2 how the ionization equilibrium is attained for oxygen and iron ions when the electron temperature is raised from 100 eV to 300 eV and 600 eV[4]. For oxygen the fully ionized ion OIX is formed only in a later stage. In the intermediate stage OVII and OVIII are overabundant in comparison with the equilibrium case.

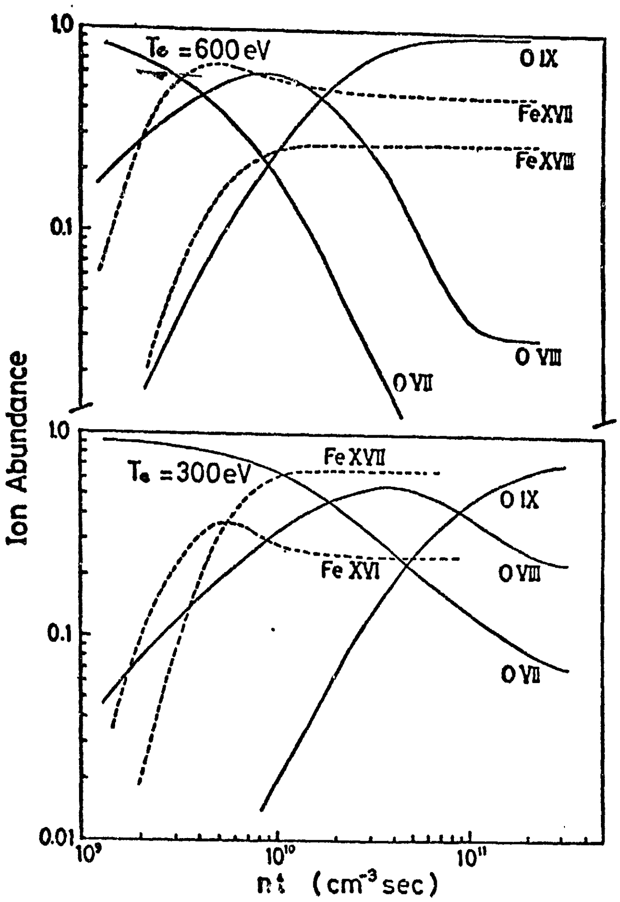

Fig.2. The time dependences of ion abundances when the electron temperature is raised from 100 eV to 600 eV and 300 eV. The abscissa is represented in units of nt (cm^{-3} sec), where n is the electron density.

Since partially ionized ions are left at such a high temperature, the line emission therefrom gives a much greater contribution to the radiation loss than in the equilibrium case. The photon yields in two energy bands, L(150-300 eV) and M(500-800 eV) taking the energy resolution of a proportional counter into account, are compared for ionizing and equilibrium plasmas in Figure 3.[4] A deviation is small for the L-band, since lines respensible for this band are mainly of the L- and M-shells of metallic elements; they reach an equilibrium rather quickly because of a large contribution of dielectronic recombination.

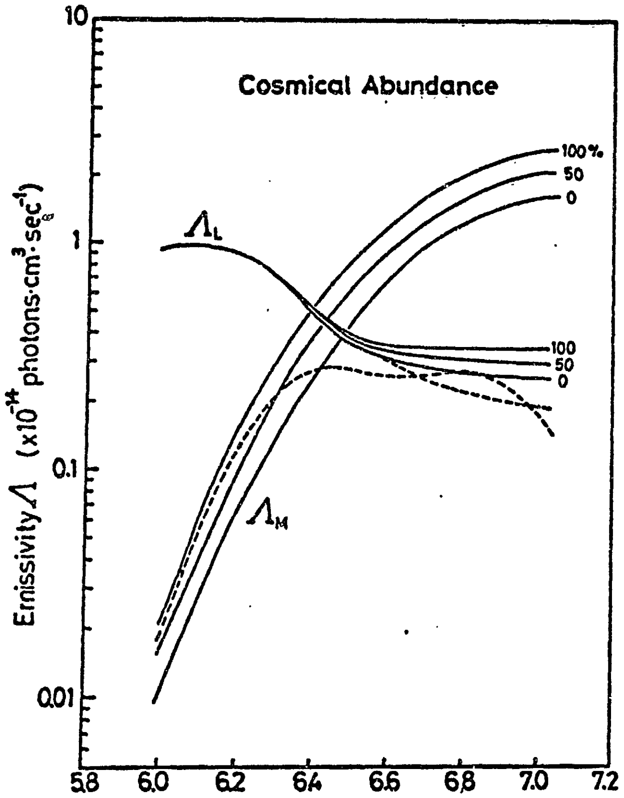

Fig.3. The photon emissivity per ion pair versus temperature. Λ_L and Λ_M are the emissivities of photons in the energy ranges 150-300 eV and 500-800 eV, taking the energy resolution of proportional counters into account. No ionization equilibrium of oxygen ions is assumed, but the relative abundances of OVII with respect to the abundances of OVII and OVIII are assumed to be 0, 50 and 100%. The dotted lines represent Λ_L and Λ_M for ionization equilibrium.

ATOMIC PROCESSES IN DENSE PLASMA

A plasma formed by laser irradiation of a solid body is very dense, and atomic processes taking place in such a dense plasma are significantly different from those in a thin plasma. Since irradiation lasts for a very short period, the plasma is almost purely ionizing in the initial stage. The probability of radiative deexcitation is extremely small compared with that of excitation and ionization. The average time for bremsstrahlung is long compared with the initial compression time. Even if radiation is emitted, radiated photons are quickly absorbed either by bound-free or by free-free absorption. As the target is highly ionized and then expands, it begins to emit radiation. The plasma in this stage is recombining.

In a dense plasma bound levels are shifted, since the Coulomb field of a nucleous is appreciably shielded by near-by electrons. The Debye length

$$d = 6.9 \times 10^{-7} (T_7/N_{21})^{1/2} \text{ cm}, \tag{2}$$

where T_7 and N_{21} are the electron temperature and density in units of 10^7K and 10^{21} cm^{-3}, respectively, becomes comparable to the average orbit radius

$$a = 5.3 \times 10^{-9} \frac{1}{2} [3n^2 - \ell(\ell + 1)]/z \text{ cm}, \tag{3}$$

where n and ℓ are the principal and angular momentum quantum numbers, respectively, and z is the ionic charge. Hence outer orbits otherwise bound become unbound.

The effect of Debye shielding considered above is based on the static approximation. The shielding field oscillates at the plasma frequency

$$\omega_p \simeq 2 \times 10^{15} N_{21}^{1/2} \text{ rad s}^{-1}. \tag{4}$$

Since this is comparable to the orbital frequency

$$\omega_n \simeq 3 \times 10^{16} z^2/n^2 \text{ rad s}^{-1}, \tag{5}$$

the line broadening is very large. The field strength due to plasma waves is

$$F_p \simeq 2 \times 10^9 (N_{21} T_7)^{1/2} \text{ V cm}^{-1}, \tag{6}$$

which is compared with the Holtsmark field strength

$$F_H \simeq 3.8 \times 10^7 N_{21}^{2/3} \text{ V cm}^{-1}. \tag{7}$$

This suggests that the coupling of plasma waves with orbital motion is important. The electrostatic field of plasma waves would give rise to considerable Stark broadening and may, in some cases, intermix discrete levels.

If one deals with radiation, higher bound levels are regarded as belonging effectively to continuum, because the collisional ionization rates for such levels are greater than the radiative deexcitation rates. Namely, these levels merge into the continuum and do little participate in bound-bound emission. The principal quantum number for this threshold is estimated as[5]

$$n_t \simeq 0.5 z^{12/27} (T_7/N_{21}{}^2)^{1/17}. \tag{8}$$

Hence only a few levels are regarded as being practically bound.

Excitation to levels of $n > n_t$ should therefore be considered as ionization. This effectively increases the ionization rate. Levels of $n > n_t$ do not take part in dielectronic recombination, thus resulting in a significant reduction of the dielectronic recombination rate. On the other hand, electrons of $n > n_t$ take part in three-body recombination, thus increasing the three-body recombination rate. The relative importance of these two opposite effects is very sensitive to the ionic charge.

The above considerations indicate that novel fratures arise in atomic processes in a dense plasma. This will open a new area of atomic physics to be explored in coming several years. The development of plasma physics and its application to the inertial confinement fusion will depend on the achievement of atomic physics. These two branches of physics cannot be separate from but should be incorporated with one another in such a high density plasma.

The author thanks Drs. T. Fujimoto and T. Kato for their cooperation in preparation for the manuscript.

REFERENCES

1. T. Kato, IPPJ-AM-4 (1978).
2. S. Hayakawa and T. Kato, JAERl-M 8060 (1979).
3. D.E. Post, R.V. Jensen, C.B. Tarter, W.H. Grasberger, and W.A. Lokke, Atomic Data and Nuclear Tables, 20, 397 (1977).
4. S. Hayakawa, T. Kato, F. Nagase, K. Yamashita, and Y. Tanaka, Publ. Astr. Soc. Japan 31, 71 (1979).
5. H.R. Griem, Plasma Spectroscopy, Mc-Graw-Hill, New York, 1964.

THE INTERNATIONAL PROGRAMME OF ATOMIC AND MOLECULAR DATA FOR FUSION

Konstantinos Katsonis, Francis J. Smith

International Atomic Energy Agency, Nuclear Data Section
Atomic and Molecular Data Unit
Kärntnerring 11, P.O.B. 590, A-1011 Vienna, Austria

The Atomic and Molecular (A+M) Data for Fusion programme of the International Atomic Energy Agency was recommended by the First Advisory Group Meeting on A+M Data for Fusion held at Culham Laboratory, U.K., in November 1976. At that meeting it was recognized that the needs for A+M data for the development of fusion research and technology are so large that any one Member State cannot adequately fulfil these needs for the whole world. Thus, not only was it deemed necessary to coordinate the collection of the requirements and the acquisition of the required data on atomic and molecular processes, but also to create a network of data centres for the dissemination of these data to the fusion community. The meeting recommended the formation of an international network of data centres for the compilation and dissemination of atomic and molecular data required for fusion, and that the IAEA Nuclear Data Section be given the responsibility to establish and coordinate this network. In accordance with these recommendations, the Atomic and Molecular Data Unit, within the IAEA Nuclear Data Section, was established for a trial period of two years (1977-1978) beginning January 1977. A Joint IFRC/INDC (International Fusion Research Council/International Nuclear Data Committee) Subcommittee on A+M Data for Fusion was formed to supervise its activities and review its programme.

Following the recommendations of the IFRC/INDC Subcommittee at its first meeting at Culham in November 1976, the initial tasks of the A+M Data Unit were as follows:

- compilation, publication and distribution of a quarterly bulletin on newly measured or calculated fusion-related A+M data and associated information;

- creation and publication of an international index of references to atomic collision data; and

- formulation of a common system for the exchange of bibliographic and numerical A+M data between existing or planned A+M data centres.

To assist the Atomic and Molecular Data Unit in accomplishing these tasks, the First Meeting of the A+M Data Centre Network was held in Vienna in May 1977. The specific accomplishments of this meeting were the establishment of agreements for the cooperation between existing A+M data centres and groups and the IAEA Nuclear Data Section/A+M Data Unit with regard to the Quarterly Bulletin on Atomic and Molecular Data for Fusion, and the exchange of evaluated atomic collision data.

Immediately following this meeting, a Second Meeting of the Joint IFRC/INDC Subcommittee was held; a third and fourth meeting of the same subcommittee were held also in Vienna in April and September 1978. In all three meetings the Subcommittee reviewed the progress which the IAEA programme on A+M Data for Fusion made during the trial period 1977–1978 and discussed the future development of the programme. The programme was judged to be proceeding according to the recommendations except a delay in the completion of the Index to Atomic Collision Data; the future programme including the continuation of the International Bulletin on Atomic and Molecular Data for Fusion, the completion of the Index, the creation of an evaluated A+M Data File for Fusion and the coordination of the network of data centres was supported. It was the judgement of the Subcommittee that the response from the scientific fusion community has been very positive, that the programme is needed, and that the IAEA is uniquely qualified to implement this programme.

In 1979 the A+M programme moved into a year of evaluation. In the course of this year the A+M programme is expected to be approved and become a regular part of the Agency's programme beginning January 1980.

The development of the Bulletin and its production is continuing; nine issues have been issued so far, the last covering the period ending on 1 July 1979. Up to now, the Bulletin has been the main achievement of the A+M Data Unit. It is mailed regularly to more than 750 scientists, laboratories or libraries and it has received favorable response and constructive criticism from the fusion community.

The preparation of the Bibliographic Index to Atomic Collision Data has also been a big part of the A+M Data Unit effort. It is expected to be published at the end of this year. It will contain over 50.000 indexation lines, representing about 10.000 references, and incorporating bibliographic data from the most active national data centres in this field (in France, Japan, UK, USA, USSR) and the collision references appearing in the last ten issues of the Bulletin. The years of coverage are 1950 – 1979 with some additional references from prior years.

In selecting the material that might be relevant to fusion a number of problems arose for both the Bulletin and the Index in connection with

i. the topics that have to be considered

ii. the concrete physical processes in each topic, and the corresponding energy range

iii. the particles or materials involved.

In the Bulletin these problems were related to the selection of papers from the current literature, and in the Index to the elimination of references not relevant to fusion from the reference files supplied by the contributing centres.

The topics to be included in the Bulletin were discussed "in extenso" during the first A+M Data Centre Network meeting (Vienna, May 1977). The following topics were retained:

1. Structure and spectra
2. Atomic and molecular collisions
3. Macroscopic plasma properties and plasma diagnostics
4. Particle-surface interactions.

The processes corresponding to the first two topics are shown in Table I. These are the processes used in the indexation of data appearing in the Bulletin (1. and 2.) and to appear in the Index (2.).

Although bibliographic data from particle-surface interaction are included and indexed in the Bulletin, the considered processes were not the result of an international agreement. It is expected that problems related with topics 3. and 4. not included in Table I will be discussed at the Second Advisory Group meeting and at the Second A+M Data Centre Network meeting, to be held in Paris from 19 to 22 May 1980 and from 23 to 24 May 1980 correspondingly.

An essential part of the preparation of the Bulletin is the choice of data and references to be included in the Bulletin. This choice is based on a criterion which acts as a guide to the editors but is not used rigidly in the production of the Bulletin; each paper is judged on its own merits. However, to ensure that as few errors as possible are made, the criterion has been built into a computer subroutine, appropriately named "Procrustes", which separates data apparently relevant to fusion from data which are not relevant to fusion. This is used to print a warning to the editors of the Bulletin when data is outside the guidelines defined by the criterion. The editors can then check that no error was made. The same subroutine is also used in the preparation of the Index. In that case, however, because of the total amount of information to be treated, it is not possible for the editors to check every line. The subroutine is therefore used to cut out automatically data apparently not relevant to fusion.

To classify the many different processes it is convenient to first separate the involved particles into different classes. The separation now used is shown in Table II. For convenience, a photon was taken to be a particle and, being unique, forms a class of its own. Similarly, the electron made a second class of particle. Those atoms, and their ions, which can predominate in a fusion plasma formed the third class, i.e. H, D. T. Because helium ions are produced at several MeV following a fusion reaction, helium is in a separate class. This allows a choice of the corresponding upper limit of the energy of collision with other particles. The molecules (or their ions) which may occur at the cool edge of plasma form two classes according to their frequency of occurrence. The list of atomic impurities consists of atoms and their ions with widely varying frequencies. Oxygen and carbon are, by far, the most abundant impurities. If a carbon limiter is to be used, their abundances may be comparable and they are, therefore, classified together, separately from other impurities. The rest of the atomic impurities are separated into two groups, "impurities" and "less common impurities", as shown in Table II. The remaining atoms can be separated into two groups: (1) atoms related to the impurities in some way which might allow data for these atoms to be used to estimate data for the impurity atoms through their position in the Mendeleev Table or through their position in an isoelectronic series, (2) atoms not usefully related to the impurity atoms, e.g. the lanthanide and actinide series of atoms, and very heavy atoms taken to be those with atomic numbers greater than that of Pb (Z=82). The resulting classification scheme is shown in Table II.

For structure and spectra data, all of the atoms and molecules in classes 3 to 8 and in class 10 are retained, being possibly present in the plasma; related atoms and molecules of the class 9 are also retained. For the special case of interatomic potentials, the same criterion as for collision data was adopted.

The choice made for collision data is shown in the matrix of possible collisions between the different classes given in Table III. Collisions between one minor constituent and another have been left out, as they cannot affect the plasma. An exception to this is collisions between the class of O and C with itself. This was a marginal decision, as such collisions can have little effect on the plasma, except perhaps resonant charge exchange. Collisions between the primary molecules and all other classes are included because of their importance for beam injection.

The upper limit of the energy range that might be of interest to fusion is included in Table III; the accepted energy range E is either the energy of the colliding photon or electron, or the center-of-mass energy of the colliding heavy particles. The highest energy for collisions between photons and other classes has been set at 30 keV. This is just above the ionization potential, about 25 keV, of the impurity atom Mo. Higher energy photons produced by collisions of runaway electrons with the surface are too infrequent and have too low cross sections to be included. There is no lower energy limit for photon collisions. The energy range for collisions between electrons and other particles has been set at 0.1 eV to 100 keV, representing the limits of the energies of thermal electrons. Runaway electrons can have much higher energies, but these have very low cross sections and are not frequent enough to be significant for plasma processes. Because the primary atoms and molecules can occur in high energy beams used for plasma heating and fueling, the high energy limit for collisions between these and the other heavy particles has been set above the highest thermal energy, at 500 keV. The lower energy limit is the thermal limit: 0.1 eV. Since helium ions are produced with several MeV energy during a fusion reaction, the limit of the collision energy between He and all other heavy particles has been set at 5 MeV. The lower thermal limit is 0.1 eV. Collisions between the class of C and O with itself have only thermal energies in the plasma; the corresponding limits have, therefore, been set at 0.1 eV and 100 keV.

TABLE I. CONSIDERED PROCESSES

1. Structure and Spectra

1. Spectral identification; Energy levels; Ionization potentials; Wavelengths
2. Transition probabilities; Oscillator strengths; Lifetimes
3. Broadening: Lineshapes and shifts
4. Polarisabilities; Electric moments
5. Interatomic potentials

2. Collisions

A. Involving photons

1. Total absorption, Scattering
2. Elastic scattering (Thomson, Rayleigh)
3. Inverse Bremsstrahlung
4. Photoionization
5. Photodetachment
6. Photodissociation

B. Involving electrons

1. Total scattering, momentum transfer
2. Elastic scattering
3. Excitation
4. Deexcitation
5. Ionization
6. Recombination
7. Attachment
8. Detachment
9. Dissociation
10. Bremsstrahlung

C. Between heavy particles

1. Total scattering
2. Elastic scattering
3. Excitation
4. Deexcitation
5. Ionization
6. Recombination
7. Charge transfer
8. Detachment
9. Dissociation
10. Association
11. Interchange reactions

TABLE II. CLASSIFICATION OF PARTICLES

(all ions of relevant atoms and molecules are included in each class)

Class	Name	Constituants
1	Photon	$h\nu$
2	Electron	e^-
3	Primary Atoms	H, D, T
4	Helium	He
5	Primary Molecules	H_2, H_3^+ and variations with one or more H atoms replaced by D or T
6	Common Impurities	C, O
7	Impurities	B, N, Al, Si, P, S, Cl, Ti, V, Cr, Fe, Ni, Zr, Nb, Mo, Ta, W
8	Less Common Impurities	Li, Be, F, Ne, Na, Mg, Ar, K, Ca, Sc, Mn, Co, Cu, Zn, Kr, Ag, In, Xe, Cs, Pt, Hg, Au
9	Related Atoms	Ga, Ge, As, Se, Br, Rb, Sr, Y, Tc, Ru, Rh, Pd, Cd, Sn, Sb, Te, I, Ba, Hf, Re, Os, Ir, Tl, Pb
10	Molecules	H_2O, OH, H_3O^+, O_2, CO_2, CO, He_2^+, HeH^+, CH_4, CH_3, CH_2, CH and variations with one or more H atoms replaced by D or T
11	All Other Atoms or Molecules	

TABLE III. DATA TO BE ACCEPTED AS RELEVANT TO FUSION*

Class	3 Primary Atoms H, D, T $<100\%$	4 Helium He $<15\%$	5 Primary Molecules H_2, H_3^+, D_2, etc. $<5\%$	6 Common Impurities C, O $<5\%$	7 Other Impurities B, N, Al, etc. $\ll 1\%$	8 Less Common Impurities Li, Be, F, etc. $\ll 0.1\%$	9 Related Atoms Ga, Ge, etc.	10 Molecules H_2O, OH, etc. $\ll 1\%$
1	E <30 keV	E <30 keV	E <30 keV	E <30 keV	E <30 keV	E <30 keV	E <30 keV	E <30 keV
2	E <100 keV	E <100 keV	E <100 keV	E <100 keV	E <100 keV	E <100 keV	E <100 keV	E <100 keV
3	E <500 keV	E <5 MeV	E <500 keV	E <500 keV	E <500 keV	E <500 keV	E <500 keV	E <500 keV
4	-	E <5 MeV	E <5 MeV	E <5 MeV	E <5 MeV	E <5 MeV	E <5 MeV	E <5 MeV
5	-	-	E <500 keV	E <500 keV	E <500 keV	E <500 keV	E <500 keV	E <500 keV
6	-	-	-	E <100 keV	None	None	None	None
7 - 11	None	None	None	None	None	None	None	None

* Provided that (1) the energy range includes values over 0.1 eV, and
(2) differential cross sections are over a wide range of angles.

CORPUSCULAR DIAGNOSTICS OF HOT PLASMA

V.V.Afrosimov, M.P.Petrov

A.F.Ioffe Physico-Technical Institute
Academy of Sciences of the USSR, Leningrad 194021,USSR

Corpuscular plasma diagnostics is based on the analysis of particles emitted by plasma ("passive" diagnostics) or injected into plasma ("active" diagnostics) for determination of the plasma parameters. Application of this diagnostics technique has been extended very rapidly in the recent years, mainly for quasistationary systems and first of all for tokamaks. Corpuscular diagnostics turned out to be the most effective way to study the ion component of plasma and especially hydrogen ions and atoms. For tokamaks the main part of information on the energy and mass-balance of hydrogen ions and atoms is obtained using corpuscular diagnostics.

Corpuscular diagnostics well satisfies the specific requirements which should be fulfilled in the investigation of hot plasma. Firstly, corpuscular diagnostics (both passive and active) does not disturb plasma and is practically contactless. Secondly, it is practically a direct method because it deals either with the particles of the plasma itself or with particles formed in binary collisions between the "probing" particles, injected into plasma, and the plasma particles. Therefore for plasma parameter determination only the data of atomic and electronic collision processes are necessary. It is important that corpuscular diagnostics is possible without a priori plasma models.

Among the corpuscular diagnostics methods the most widely used ones are those based on the analysis of neutral, to wit, hydrogen atoms. The reason of this is that the cross sections of processes involving hydrogen atoms are well known and, besides, neutrals easily penetrate the electromagnetic fields surrounding the plasma and can be analyzed outside the plasma installation. On the other hand, the hydrogen atoms exist in any of contemporary fusion machines in spite of rather high parameters of the plasma temperature and density.

The main mechanism supporting the existence of neutral hydrogen particles in the majority of plasma installations is the income of atoms from the walls. The most probable process for hydrogen atoms in the hydrogen plasma is the resonant charge exchange on protons. Due to the charge exchange of slow atoms on fast protons fast atoms appear in plasma. These fast atoms can penetrate into the central hot region of the plasma where, in their turn, undergo charge exchange with hot protons. This "relay-race" charge exchange mechanism leads to the formation of radial distribution of neutrals and to the possibility of using corpuscular diagnostics for investigation of both the peripheral and central regions of the plasma column. It is important that the ratio between the fluxes of atoms from and to the plasma given by albedo A increases with increasing in the plasma temperature and at $T \gtrsim 600-700$ eV is as high as $A = 0,6 - 0,7$. Thus, the tokamak plasma is always a source of hydrogen atom fluxes which can be used for "passive" corpuscular diagnostics.

There are at least two important problems which can be solved by the analysis of atoms emitted by plasma: a) determination of ion temperature using energy distribution of these atoms and b) elucidation of mass and energy balance of the ion component and determination of the role of different channels in plasma ion energy losses - using the absolute value of an atomic flux from the plasma.

For the atomic flux analysis different types of analyzers have been developed [1,2]; as an example a 5-channel analyzer is shown in Fig.1. Plasma radiation is collimated and penetrates a chamber G filled with gas where part of atoms is transformed into ions due to stripping. These ions are analyzed in mass by the magnet M and in energy - by the condensers $C_1 - C_5$ and finally registered by five separate counters. Thus, such an analyzer enables to obtain the intensity of the flux for atoms with definite mass and for 5 different regions of energy, i.e. energy distribution of atoms during one pulse of the plasma installation. The possibility of such measurements is very important for the separation of hydrogen atoms from deuterium and impurities and for the determination of ion temperature and energy balance in large tokamaks with long intervals between pulses. It should be emphasized, that for the correct determination of atomic flux parameters using the amount of registered secondary ions a careful calibration of the analyzer is necessary. This calibration is performed on special installations using monokinetic atomic beams with a definite energy and intensity. Unfortunately, several investigators underestimated the importance of calibration which led to mistakes in neutral corpuscular diagnostics.

A typical example of energy spectra of atoms is shown in Fig.2 [6]. The energy spectrum of hydrogen atoms in plasma is closely connected with the spectrum of protons. This is due to the fact that the resonant charge exchange occurs practically without transfer of kinetic energy and scattering of the interacting particles. As a result, an atom formed in the resonant charge exchange has the same magnitude and direction of velocity as the primary plasma proton.

The resonant charge exchange cross section for hydrogen is $\sigma_{c.e.} \sim 10^{-15}$ cm^2, which leads to a rapid "energy mixing" between hydrogen atoms and protons. So the slop of the linear part of distribution in Fig.2 reflects ion temperature of the hottest, central region of the plasma column. The rise of the spectra at lower energies is connected with the emission of atoms from the peripherical plasma regions with lower temperatures. A solid line in Fig.2 represents calculated energy spectra which coincide well with the experimental results.

Measurements of the atom flux time-dependence give information about ion temperature changes during discharge in plasma installations. Comparison of neutron yields with ion temperatures measured using the energy spectra of emitted hydrogen atoms enables us to ascertain whether the neutrons are of thermonuclear origin or not.

General regularities of the ohmic heating of hydrogen ions in Tokamaks have been studied using corpuscular diagnostics [3-7]. It has been shown, that the ion temperature corresponds to Artsimovitch"s formula, i.e. to the Coulomb energy transfer from electrons to ions and to the ion cooling via neoclassical thermoconductivity. The simultaneous determination of the ion temperature and the hydrogen atom concentration from the data on emitted atom fluxes makes it possible to obtain energy confinement time, and the role of different energy loss channels: thermoconductivity, diffusion, charge exchange. Fig.3 shows an example of the radial distribution of relative intensities of the channels. In the central region thermoconductivity plays the main role; near the walls charge exchange becomes important.

Corpuscular diagnostics is practically the only method of observing and studying local-trapped particles. The behaviour of these components of plasma can be investigated using the anisotropy of atom fluxes obtained from passive corpuscular diagnostics measurements. It turned out that in Tokamak T-4 at T_i = 0,7 keV the local-trapped ions translate about half of ion energy losses.

The concentration of atoms n_0 in the central region of the plasma must principally decrease with increasing of the plasma density and the Tokamak dimensions. In Alcator, for example, it should be $n_0 \sim 10^3$ cm^{-3}. But, as has been shown recently, real n_0 is about 10^3 times higher [8]. This is caused by the creation of atoms due to radiative electron-proton recombination [9] (Fig.4). This result is important, because it means that it is impossible to "burn out" all the neutrals in the central region of plasma and in any case n_0 cannot be less than 10^{-7} - 10^{-8} of plasma concentration. At the same time it means that the passive corpuscular diagnostics can be used also for the future types of Tokamaks.

The simplest type of the active corpuscular diagnostics is neutral beam-probing of the plasma with the measurements of ion concentration averaged along the beam path in the plasma using beam intensity attenuation [10]. Recently such a technique has been used with simultaneous probing of the plasma column along different chords by many (11) neutral beams. This multi-beam plasma probing provides a high spatial and time resolution and is especially convenient for the investigation of confinement and diffusion at the plasma heating using its compression by magnetic field [11].

The possibility to separate H° and D° atoms was used also for direct study of the hydrogen ion diffusion in Tokamak T-4 plasma [12]. A short pulse of deuterium gas was injected in hydrogen plasma. Time dependence of fast D° fluxes appearing after such an injection were studied in different local regions along the toroidal plasma column. The diffusion time of deuterium obtained from these dependencies was found as $\tau \sim 20$ msec.

At present the measurements of local plasma parameters are becoming more and more important for a detailed analysis of processes in hot plasma. Fig.5 shows a setup of instruments for the plasma local parameter diagnostics which are developed and applied by our lab at Ioffe Phys.Techn.Inst. (Leningrad) [13]. A narrow, intensitive monokinetic beam of H or He atoms for plasma probing is produced by an injector. Local values of ion temperature are measures in two ways: a) by determining the energy spread of the atoms scattered on moving ions at a fixed angle [14,15](using analyzer I), b) by determining the energy distribution of the atoms, formed in charge exchange of plasma ions on probing beam atoms which play role of an artificial atomic target[16] (using analyzer II). Furthermore, the instruments shown in Fig.5 give possibility to register radiation of impurity ions which is caused by the charge exchange of these ions on beam atoms [17] (X-ray spectrometer). The locality of measurements is determined by the volume formed by the crossing of the probing beam and the regions visible from the analyzers. Fig.6 shows radial ion temperature distributions obtained by charge exchange of plasma hydrogen ions on deuterium D° atoms of probing beam [13].

Impurity ion diagnostics is a combined corpuscular spectroscopical one. It is based on the fact that for multi-charged ions the charge exchange with H° atoms has a large cross-section $10^{-15} - 10^{-14}$ cm^2 and that an electron is captured practically only onto excited levels of an ion:

$$\vec{H}^{o} + A^{+z} \rightarrow \vec{H}^{+} + A^{+(z-1)*} \rightarrow \vec{H}^{+} + A^{+(z-1)} + \hbar\omega$$

By observing an increase in intensity of the characteristic lines $A^{+(z-1)}$ of ions from different regions along the injected H^{o} - beam, one can measure absolute local concentrations of A^{+z} ions. The advantage of this new impurity diagnostics [17], besides locality, is the application of a definite mechanism of ion excitation and the possibility to study bare nuclei in plasma which are inaccessible for observation in the usual spectroscopical way. This "combined" impurity diagnostics was used for C^{6+} nuclei diagnostics in T-4 and an increase of L_{α} - line of C^{5+} was observed at injection of H^{o}-beam (8 keV, 10 mA/cm^2). It was found [18], for example, that in the central region of T-4 the concentration of C^{6+} is $\sim 1.10^{11}$ cm^{-3}, i.e. 0,25% of the plasma density. The diffusion time of C^{6+} from the central region is about 20 msec, i.e. the same as for the hydrogen ions which means that impurities are not accumulated in this region during the steady-state period of discharge.

It is obvious, that for the extension of this technique to impurities of different elements and charge states a systematic investigation of the charge exchange of multi-charged ions into excited states and the radiative decay of these states are necessary.

In conclusion, one can note that corpuscular diagnostics which was developed about twenty years ago has become now the main way of studying ion heating and confinement in quasistationary systems. The recent progress of corpuscular diagnostics has shown that possibilities of this technique can be extended further and that it will play a considerable role in CTR research in future.

REFERENCES

1. V.V.Afrosimov, et al., Zh.Tekh.Fiz., 33, 205, 1963.
2. V.V.Afrosimov et al. Zh.Tekh.Fiz., 45, 56, 1975.
3. V.S.Zaverjaev et al. Fiz.Plasmy, 4, 1205, 1978.
4. L.A.Artsimovich et al., Pis'ma Zh.Eksp.Teor.Fiz., 10, 130, 1969.
5. L.A.Artsimovich et al., Pis'ma Zh.Eksp.Teor.Fiz., 11, 449, 1970; 12, 89, 1970; IV-th Europ.Conf. on Contr. Fusion a Plasma Physics, Rome, 1970, p.1 .
6. A.B.Izvozchikov a. M.P.Petrov, Fiz.Plasmy, 2, 212,1976.
7. A.B.Berlizov et al., Atom.Energiya, 43, 90, 1977; A.A. Bagdasarov et al., VII-th Int.Conf. on Contr.Fusion a. Plasma Physics, Innsbruck, 197 , IAEA-CN-37/A-2, v.1, p.35.
8. M.P.J.Gaudreau, A.I.Kislyakov, Yu.A.Sokolov, Nucl.Fu-

sion, 18, 1725, 1978; Yu.N.Dnestrovskij, S.E.Lysenko, A.I.Kislyakov, Nucl.Fusion 19, 293, 1979.
9. Yu.S.Gordeev et al. Pis'ma Zh.Eksp.Teor.Fiz., 2, 223, 1977.
10. V.V.Afrosimov et al. Zh.Tekh.Fiz., 36, 89, 1966.
11. V.V.Afrosimov et al., Pis'ma Zh.Eksp.Teor.Fiz. 28, 472, 1978.
12. V.V.Buzankin et al. VII-th Int.Conf. on Contr.Fusion a. Plasma Physics, Innsbruck, 1978, IAEA-CN-37/5-1, v.1, p.287.
13. E.V.Alexandrov et al., Pis'ma Zh.Eksp.Teor.Fiz., 29, 3, 1979.
14. V.G.Abramov et al., Zh.Tekh.Fiz., 41, 1924, 1971.
15. V.V.Afrosimov et al., Pis'ma Zh.Tekh.Fiz., 3, 10, 1977.
16. A.M.Kudryavtsev, A.F.Sorokin, Pis'ma Zh.Eksp.Teor. Fiz., 18, 486, 1973; V.V.Afrosimov, M.P.Petrov, V.A.Sadovnikov, ibid. 18, 510, 1973.
17. V.V.Afrosimov, Yu.S.Gordeev, A.N.Zinoviev, Pis'ma Zh.Tekh.Fiz., 3, 97, 1977.
18. V.V.Afrosimov et al., Pis'ma Zh.Eksp.Teor.Fiz., 28, 540, 1978; Fiz.Plasmy, 5, 987, 1979.

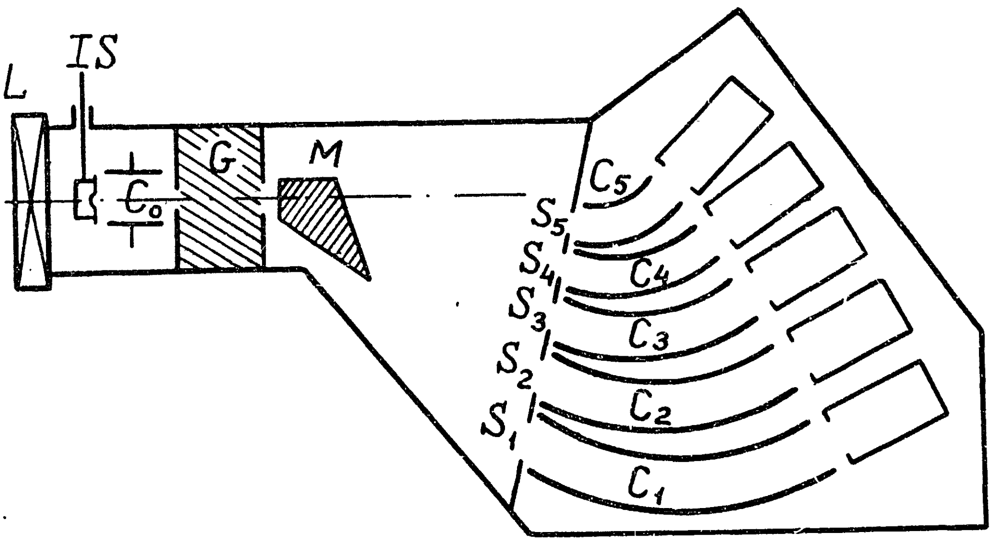

Fig.1. 5-channel analyzer of atoms emitted by hot plasma [2]

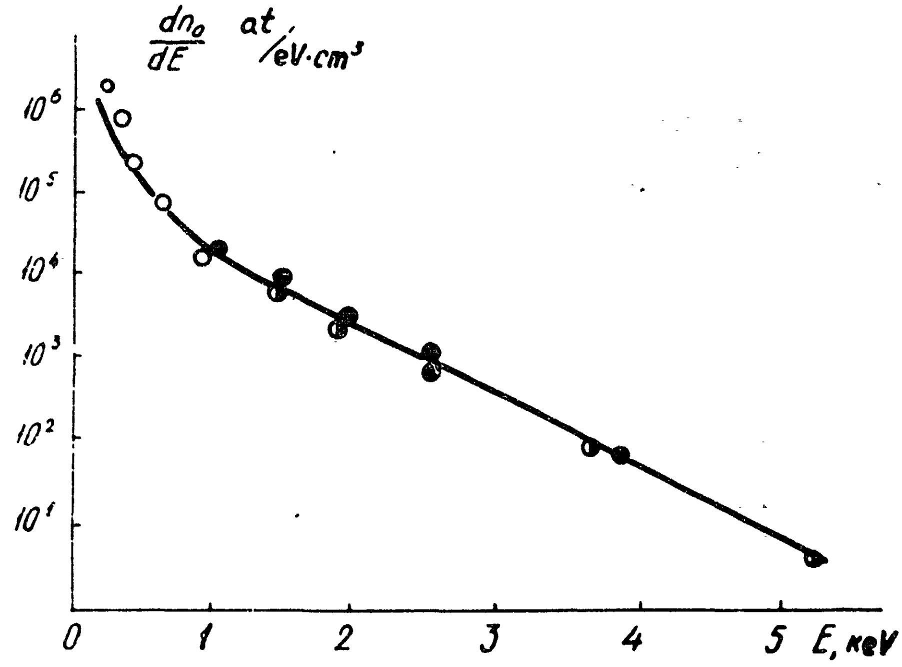

Fig.2. Energy distribution of hydrogen atoms emitted by plasma in Tokamak T-4 [6].

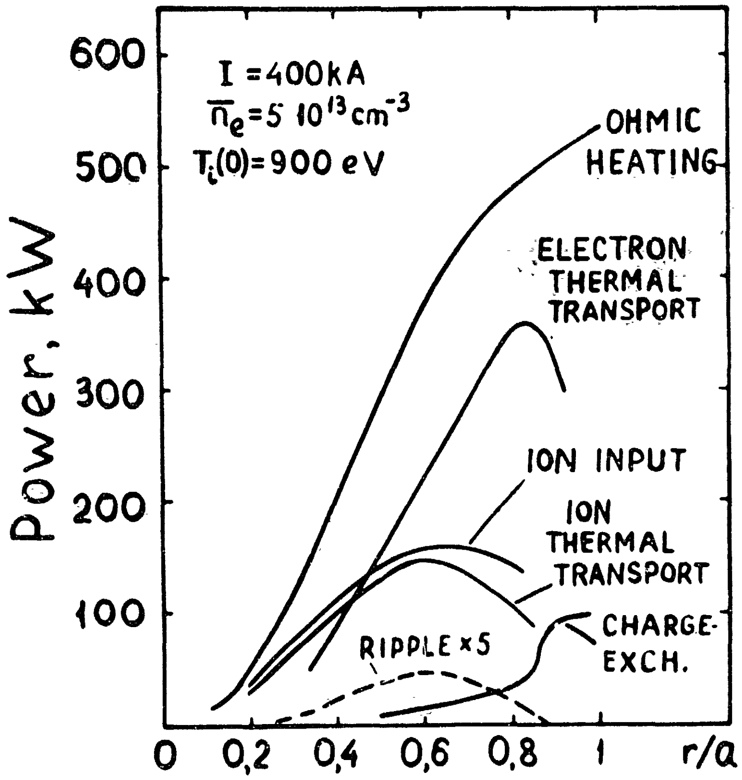

Fig.3. Radial distribution of power for different energy loss channels in Tokamak T-10 [3].

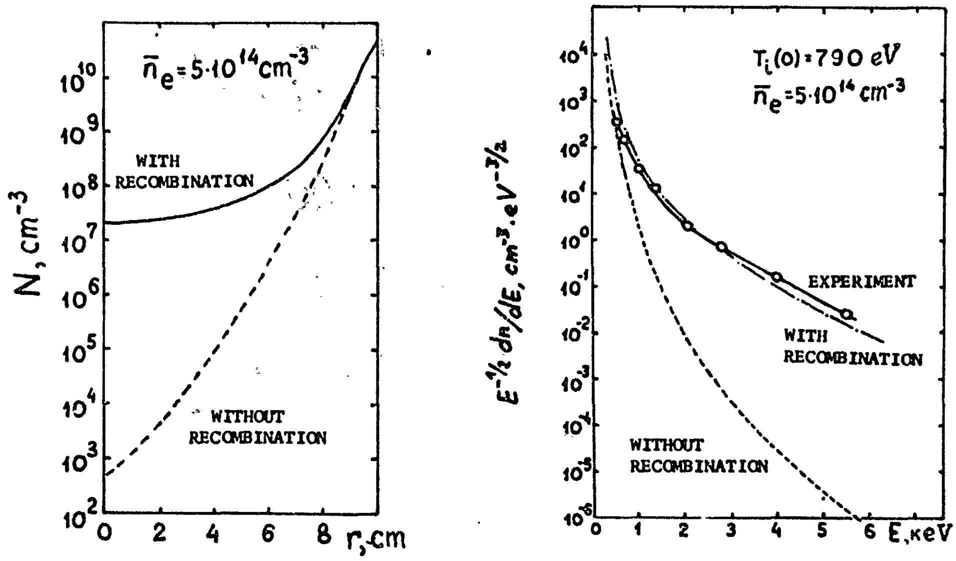

Fig.4. Concentration and energy distribution of hydrogen atoms in plasma of Alcator [8].

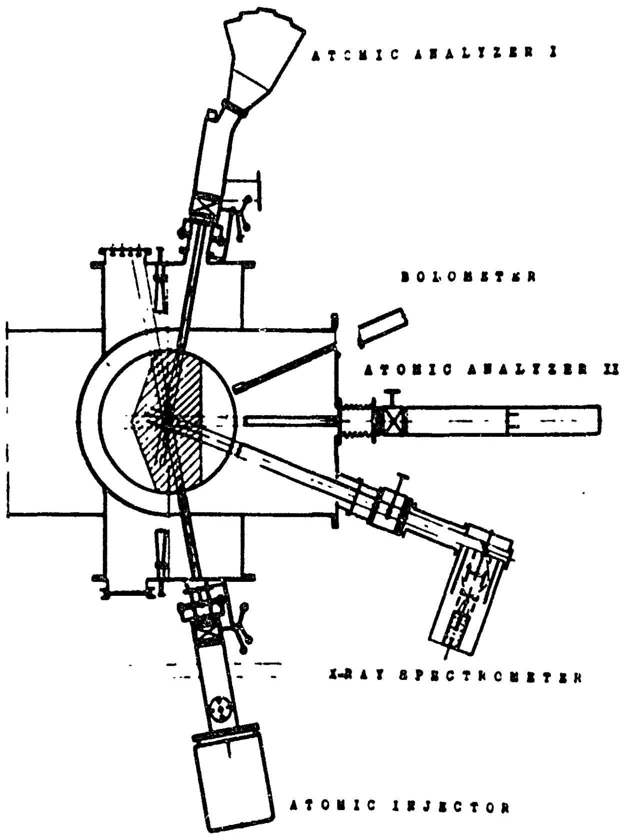

Fig.5. Set-up of instruments for combined corpuscular spectroscopical diagnostics of local hot plasma parameters [13, 18]

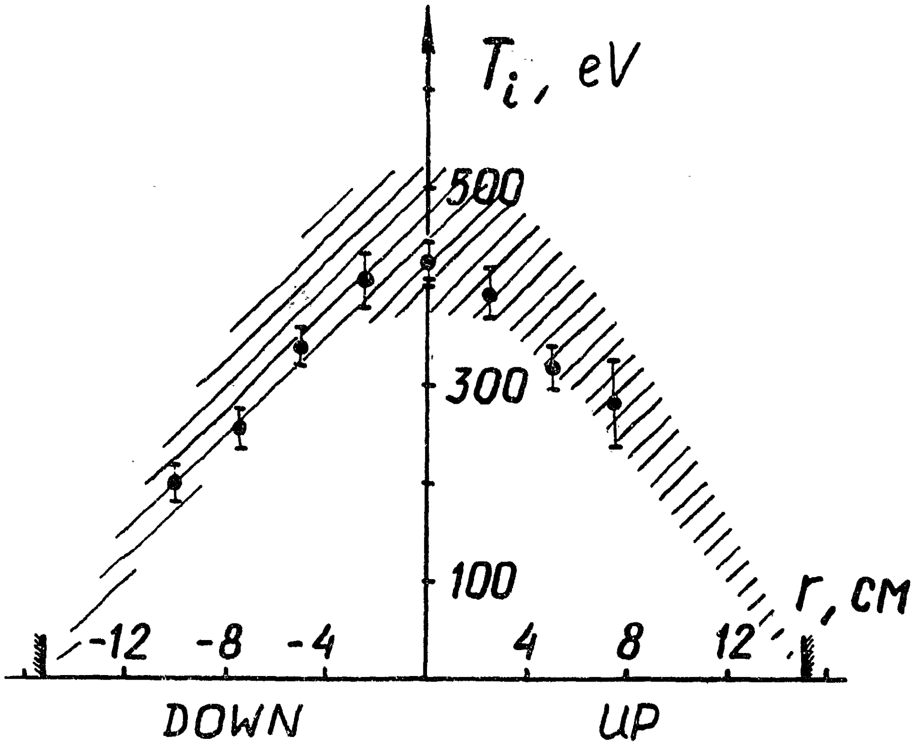

Fig.6. Local ion temperature distribution measured by charge exchange of plasma protons on deuterium atoms of probing beam [13] . Dashed region - calculations of the distribution with different assumption on plasma effective charge and neutrals concentration at plasma boundary.

PLASMA DIAGNOSTICS, ON JIPP T-II TOKAMAK

J. Fujita

Institute of Plasma Physics, Nagoya University
Nagoya 464, Japan

INTRODUCTION

An interaction of high temperature plasma with neutral atoms and molecules involves various kinds of atomic and radiative processes. In the field of tokamak research, a technique of gas-puffing in the course of discharge has been widely employed to achieve a high density plasma. The behavior of impurities in such a high density plasma is of particular interest from the view point of plasma diagnostics as well as of radiation losses from the high temperature plasma.

A detailed spectroscopic study of oxygen ions in JIPP T-II tokamak[1] has revealed that a remarkable rearrangement of the ionization states of oxygen takes place in a plasma periphery when the electron density is raised by puffing the hydrogen gas. Line radiations from oxygen ions are strongly enhanced due to the recombination processes. Calculations based on a simple model can explain the evolutions of the line radiations and also the radial profile of effective ionic charge Z_{eff} which is derived from the spatial profile of visible continuum (Bremsstrahlung).[2] The model implies a possibility of finding out the confinement times for the exygen ions of each ionization state.

EXPERIMENTAL DEVICES

JIPP T-II is a hybrid device of tokamak and stellarator, and has a major radius of 91 cm, plasma radius of 15 cm, and a toroidal magnetic field of 30 kG maximum.

The parameters of the plasma produced in tokamak operation are as follows:

line-averaged electron density	:	$1 - 7 \times 10^{13}$ cm^{-3}
electron temperature	:	400 - 1300 eV
ion temperature	:	250 - 750 eV
plasma current	:	160 kA
discharge duration	:	0.2 - 0.5 sec

Two additional heating systems are prepared and applied; a neutral beam injection heating and a lower hybrid wave heating. The third heating system, an electron cyclotron heating system is now ready to apply.

A 2 m, grazing incidence spectrometer which covers the spectral range from 15 to 1300 Å with an incident angle of 87° was used in this experiment. The plasma was observed along a chord passing through the plasma axis. In the visible region, spatial profile of the emission was measured.

EXPERIMENTAL RESULTS

Typical traces of loop voltage, plasma current, line-averaged electron density, and electron temperature are shown together with the intensity of oxygen line in Fig.1(a) for the case of strong gas puffing after the discharge reaches a steady state. The electron density certainly goes up to as high as 5×10^{13} cm^{-3}, but the cooling of plasma edge by the neutral gas causes a shrinking of plasma column and results in a disruption. On the other hand, if the plasma current is raised rapidly a little after the gas puffing (Fig.1(b)), the edge of the plasma is heated due to the skin effect, and the radial profile becomes flatter. This prevents the occurrence of the disruption, and a stable high density plasma is produced.

In a normal tokamak discharge as is in the steady state before gas is puffed, fairly high amount of 6-times ionized oxygen ions are present at the periphery because of a longer recombination time compared with a particle confinement time. The lowering of electron temperature and the increase in electron density due to gas puffing enhance the recombination of 6-times ionized oxygen. This results in a significant rearrangement of charge state of oxygen, and strong emissions from oxygen ions in lower ionization states are observed. The increments in the intensities of each resonance line (OII ~ OVI) with respect to the values at the steady state are plotted in Fig.2 as a function of time. The radiation loss caused by OVI 1032 Å in the case (a) reaches about 40 kW at 30 msec after gas puffing and amounts to about 30% of the total ohmic power input into the plasma. One can notice also that the emission from higher ionization states increases earlier and linearly with time, while that from lower ionization states shows a delayed exponential increase. These features suggest that the major part of the increase in the emission is likely due to the recombination from higher ionization states.

DISCUSSION

The rate equations have been solved in order to estimate the effect caused by the recombination from O^{6+} in the peripheral region of the plasma.

$$\frac{dN(O^{6+})}{dt} = N_{out} - \alpha_6 N(O^{6+}) + S_5 N(O^{5+}) - \frac{N(O^{6+})}{\tau_6} ,$$

$$\frac{dN(O^{z+})}{dt} = \alpha_{z+1} N(O^{(z+1)+}) - \alpha_z N(O^{z+}) + S_{z-1} N(O^{(z-1)+}) - S_z N(O^{z+}) - \frac{N(O^{z+})}{\tau_z} .$$

$$(z = 0 \sim 5)$$

Here $N(O^{z+})$ is the total number of the oxygen ions z times ionized; α_z and S_z are the recombination and ionization probabilities; τ_z is the confinement time; N_{out} is the influx rate of O^{6+} into the peripheral region to be considered.

We made a bold assumption that the O^{6+} ions are present in the peripheral region and contribute as an only source of recombination processes which take place there. That is, $N(O^{6+}) = N_{out} \cdot \tau_6$, and $N(O^{z+}) = 0$ at $t = 0$ (time of gas puffing), simply because we are interested only in the increments of O^{z+} from the values in the steady states.

With this assumption and utilizing every possible data from visible spectroscopy (location of O^{5+}) and Thomson scattering of ruby laser light (radial profiles of electron temperature and density), the evolutions of

$N(O^{z+})$, so that those of resonance radiations from each ionization state of oxygen are calculated. It is significant that only limited set of parameters for the confinement times of oxygen ions can give a solution which can explain the experimental results, both in absolute values and time histories (see Fig.2); τ_6 = 10 msec, τ_5 = 10 msec, τ_4 = 5 msec, τ_3 = 1.5 msec, τ_2 = 1.5 msec, τ_1 msec and τ_0 = 0.6 msec.

This comes from the fact that, in the steady state, oxygen ions of low ionization states are found in the shell where electron temperature is fairly high. Therefore the ionization rates are higher than the diffusion rates, and the particle balance is determined by ionization and is not strongly affected by the particle confinement. On the other hand, in the high density case, oxygens of low ionization states produced due to the recombination are found where electron temperature is low, so that all the rates of ionization, recombination and diffusion are in the same order of magnitude. This is the reason why we can determine the set of confinement times for each ionization state of oxygen from the particle balance.

OTHER TOPICS

Another interesting interaction of hot plasma with neutral gas has been found in TPD-I device. A high density helium plasma (electron density over 10^{14} cm^{-3}, electron temperature of the order of 10 eV) is produced steadily, and streams out into the plasma region. When a neutral gas is introduced into the plasma region, similar situation is realized and the three-body recombination of He^{++} to He^{+}, or H^{+} to H° in the case where hydrogen gas is introduced, is strongly enhanced. This results in a population inversion in He^{+} or H°, which suggests a possibility of developing VUV or XUV lasers.[3)]

The third example of hot plasma-neutral interaction is a neutral beam probe. When we shoot a neutral particle beam into a high temperature plasma, various kinds of atomic and radiative processes take place. The role played by the neutral particle in this case is not a cooling of plasma but a probing of the plasma.

We have developed a neutral lithium beam probe[4)] to obtain a local electron density or its fluctuations. The resonance line intensity emitted from lithium by plasma electron impact excitation is expressed as a product of beam particle density, electron density and rate coefficient for electron impact excitation. Local electron density can be obtained from this intensity measurement if the beam intensity is known, because the rate coefficient is a weak function of electron temperature above 10 eV. Details will be found in the next paper by Kodota

The idea of the neutral lithium beam probing originates in the necessity of poloidal field measurement to obtain the current distribution in tokamak plasma.[5)] This utilizes the Zeeman polarization to find out the direction of local magnetic field. When we observe the emission in a perpendicular direction to the magnetic field, π component light is linearly polarized in parallel direction to the magnetic field, and σ component in perpendicular direction. A sensitive polarimeter for the filtered π component light will give us the direction of the local magnetic field, from which one can obtain the strength of the poloidal magnetic field which is produced by the plasma current when the toroidal field strength is known.

CONCLUSION

The interaction between high temperature plasmas and neutral gases involves a great variety of atomic and radiative processes. Experimental results of spectroscopic studies on high density plasma in JIPP T-II are presented as an example. The atomic processes in high temperature plasmas find many applications in the nuclear fusion research; plasma diagnostics including plasma spectroscopy and beam probing, population inversion suggesting a realization of XUV lasers, and so on.

A close collaboration between the physicists in the field of atomic processes and the plasma physicists is strongly needed to promote these researches. The Institute of Plasma Physics, Nagoya University, is a central establishment open to the collaboration in the field of plasma physics and nuclear fusion research, so that always such collaborations are heartily welcomed.

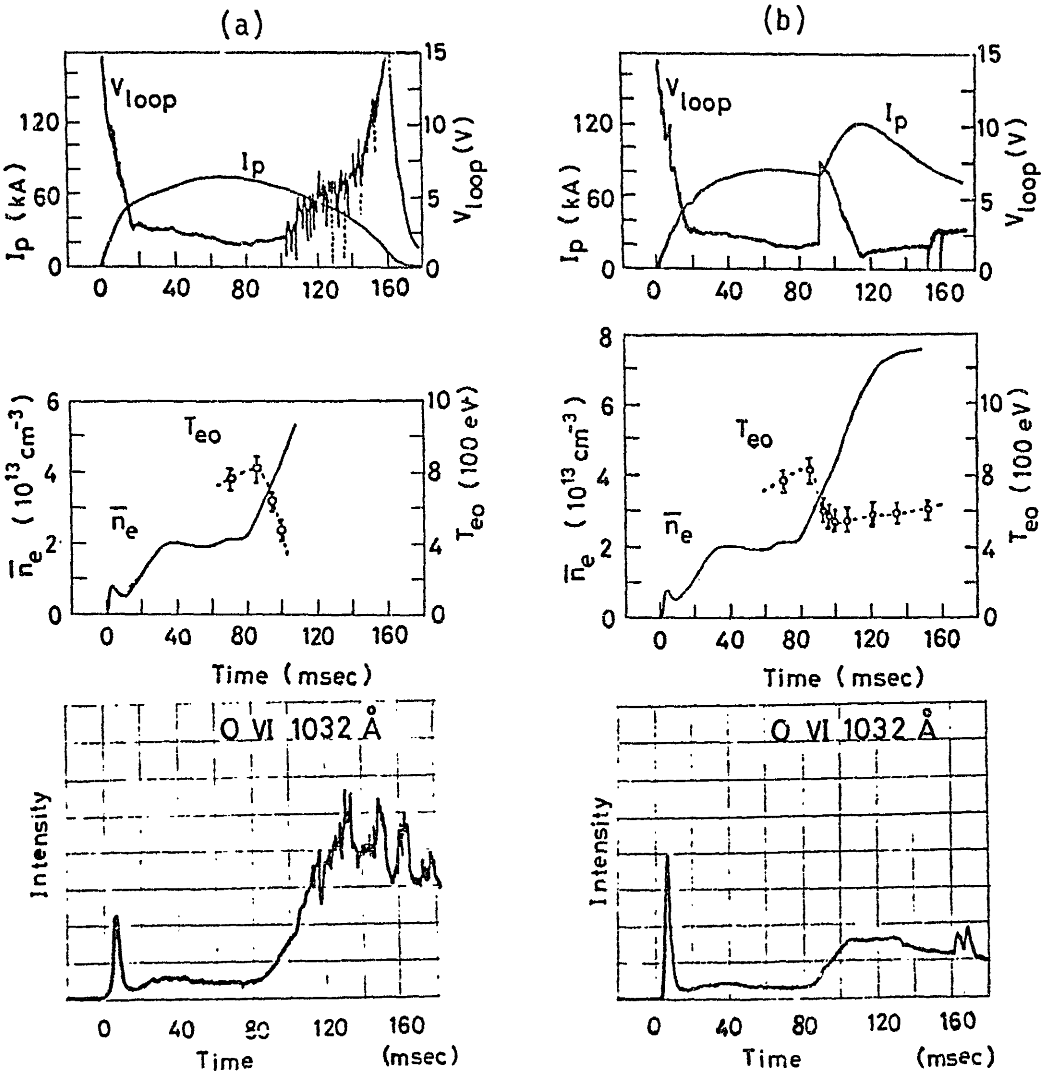

Fig.1. Time behavior of plasma parameters and radiation of O VI 1032 A line. Case (a) : with a gas puffing only, case (b) : with the gas puffing and the second current rise.

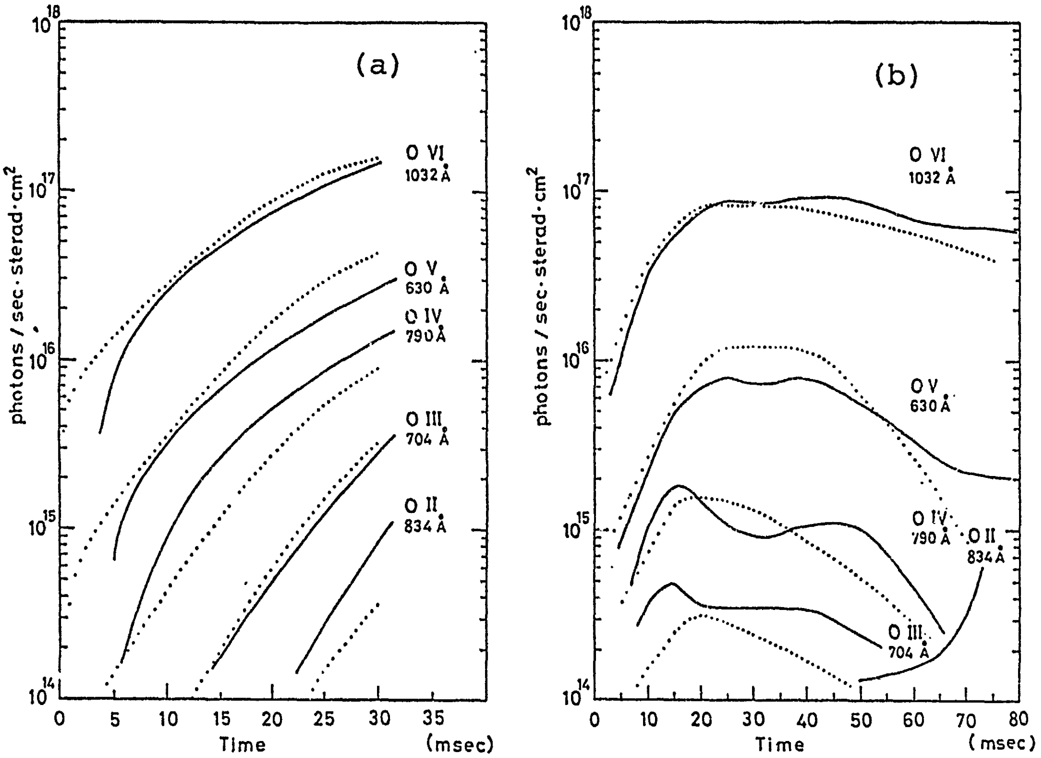

Fig.2 The behavior of increments in the intensities of each resonance line with respect to the values at the steady state after gas puffing. Solid lines show the experimental results and the calculated emissions are shown with broken line. The time t = 0 corresponds to that of gas puffing.

REFERENCES

1. J. Fujita, S. Itoh, K. Kadota, K. Kawahata, Y. Kawasumi, T. Kuroda, K. Matsuura, A. Miyahara, K. Miyamoto, N. Noda, K. Ohkubo, K. Sakurai, K. Sato, M. Sato, S. Tanahashi, Y. Terashima, K. Toi: Proc. 7th Intern. Conf. Plasma Phys. Controlled Nuclear Fusion Research, CN-37-N-2, Innsbruck, 1978.
2. K. Kadota, M. Otsuka and J. Fujita: Reports of Inst. Plasma Phys., Nagoya Univ. IPPJ-374.
3. K. Sato, M, Shiho, M. Hosokawa, H. Sugawara, T. Oda and T. Sasaki: Phys. Rev. Letters 39 (1977) 1074.
4. K. Kadota, K. Tsuchida, Y. Kawasumi and J. Fujita: Plasma Physics 20 (1978) 1011.
5. J. Fujita and K. McCormick: Proc. 6th Eur. Conf. Controlled Fusion and Plasma Phys., Moscow, 1973, p.191.

NICE PROJECT AT IPP*

Y. KANEKO

Department of Physics, Tokyo Metropolitan University
Setagaya-ku, Tokyo 158

Institute of Plasma Physics, Nagoya University
Chikusa-ku, Nagoya 464

ABSTRACT: NICE project at IPP is briefly described. Results of a preliminary experiment on symmetric resonance multiple charge transfer processes by using cryo-NICE source are presented.

INTRODUCTION

Since 1977, a research group has been organized for study of atomic processes in fusion plasma as a part of the Guest Research Program of the Institute of plasma Physics (IPP). The group consists of the following eight members;

Y. Kaneko** (Tokyo Metropolitan University)
K. Okuno (" ")
N. Kobayashi (" ")
S. Ohotani (IPP)
T. Iwai** (Osaka University)
S. Tsurubuchi (" ")
M. Kimura (" ")
H. Tawara (Kyushu University)

The main subjects of the group are to build an ion source for highly stripped ions and to make experiments on the atomic processes involving highly stripped ions, which are supposed to be important in a fusion plasma. So the project was named as "Naked Ion Collision Experiments (NICE)".

The ion source we have constructed are of EBIS type. There are various kinds of ion source for multiple charged ions; PIG, ECR, EBIS, beam-foil, laser-irradiation, etc. Each type of source has own merits and demerits. I am not willing to make comparison of each type of source here, but the reason why we have chosen an EBIS type source was that we

* Invited talk at the Nagoya Seminar on Atomic Processes in Fusion Plasma, Nagoya, 6-7 Sept. 1979.

** Guest professor of IPP

were mostly interested in the processes involing highly stripped ions in the relatively low energy region, and EBIS was considered as an suitable source for this purpose. Our source has been constructed only a few months ago, and so far we have had no time enough to make it work in the full performance, unfortunately. However, today I can present preliminary results for symmetric resonance multiple charge transfer processes, which were discovered very recently by using the cryo-NICE source.

PRINCIPLE OF EBIS

The principle of EBIS proposed by Donets[1] is as follows: When a high density electron beam is shaped with a strong magnetic field applied along the axis of the electron beam, the ions produced by electron bombardment are trapped by the space charge of the electron beam. In the direction of the electron beam axis, the ions are confined by applying a suitable potential walls. Stripping of the trapped ions proceeds through successive ionization by electron bombardment. The ions are extracted in the direction of axis by removing occasionally the potential wall.

The most important factor of the EBIS operation is

$$\tau = j \cdot t, \qquad (1)$$

where, j is the electron current density and t is the confinement time. With the larger τ, the higher charge state of ion beam is obtained. Therefore, with the higher density of electron beam j, particular charge state of ion beam can be obtained in the shorter confinement time; namely the higher intensity beam is expected for that charge state of ions.

Another important factor for the EBIS operation is the pressure. In order that the ions are trapped inside the electron beam by the space charge of the electron beam, the space charge of the electron beam must not be neutralizized by that of the ions. Namely, the following relation;

$$\sum_q q \cdot n_{q+} < n_e \qquad (2)$$

must be held, where n_{q+} and n_e are the particle density of q-hold multiple charged ions and electrons, respectively. If the background gas pressure is high, neutralization of space charge will takes place even without the sample gas introduced. A simple calculation shows the background pressure must be in the 10^{-9} Torr.

CRYO-NICE

In the first stage of the NICE Project, we constructed the ion source so-called proto-NICE, which had conventional solenoid and oil diffusion pump system. The purpose of the proto-NICE was to get know-how of the EBIS operation.

In the second stage, we have build so-called cryo-NICE. Fig. 1 shows a schematic diagram of the cryo-NICE. The cryo-NICE has a super-conducting magnet (SCM) for providing a strong and stable magnetic field. In addition to that, the reservoir of liquid helium for SCM is expected to have a function of cryogenic pump.

As mentioned before, the whole apparatus has been constructed only a few months ago, and a fine adjustment is still going on. Therefore, the full performance expected has not yet been achieved. Although the pressure inside the SCM can not be measured, the background pressure measured with an ionization gauge mounted on the vacuum chamber is 7×10^{-10} Torr.

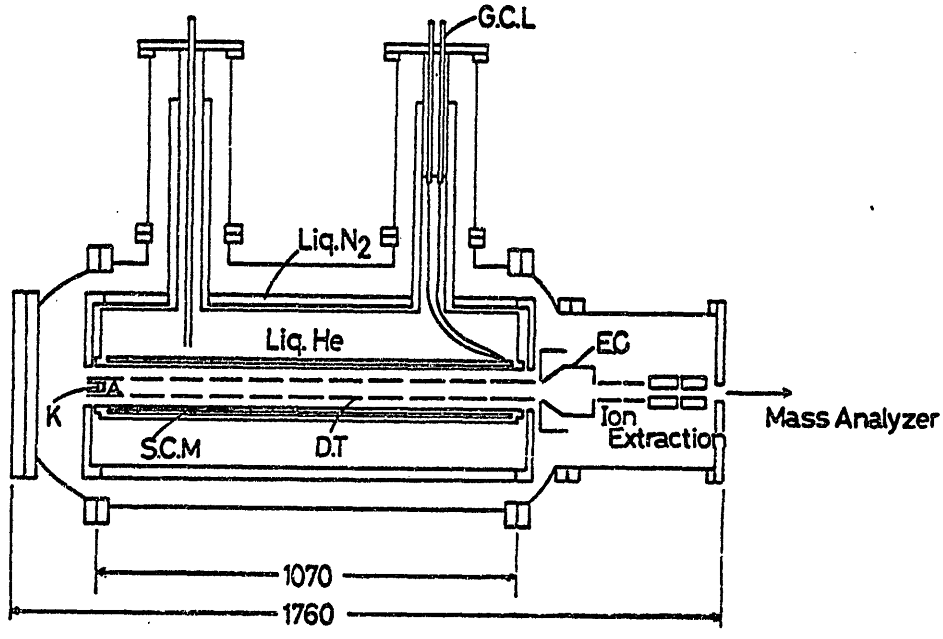

Fig. 1. A schematic diagram of cryo-NICE

CROSS SECTION MEASUREMENT OF RESONANCE MULTIPLE CHARGE TRANSFER

A preliminary measurement of the cross sections of symmetric resonance multiple charge transfer processes;

$$A^{q+} + A \rightarrow A + A^{q+}, \qquad (3)$$

have been made by using cryo-NICE. The ions extracted from cryo-NICE is mass-selected by a magnetic field of sector type, and pass through a collision cell. The beam penetrating the collision cell hits an aluminum plate, and the secondary electrons ejected from the plate are collected and multiplied with CERATRON, a channel type continuous multiplier with a corn-shaped opening. A deflector placed behind the collision cell is for the separation of charged particles from the beam. Beam intensities of the primary ions and the fast neutrals are measured by a single particle counting mode.

The entrance and exit apertures of the collision cell are 0.7 mm^{ϕ} and 2.2 mm^{ϕ}, respectively, and the length of the cell (L) is 80 mm. Target gas is introduced into the cell through a capillary tube from a reservoir, the pressure of which is monitored. From the conductance of the capillary tube and the cell apertures, the target gas pressure inside the collision cell is estimated. The target pressure is kept below 2×10^{-4} Torr. In the ordinary operating condition, the pressure of the source region is 1×10^{-9} Torr, and the outside of the collision cell is kept at 8×10^{-9} Torr by a double differential pumping with turbo molecular pumps.

For each experimental run, the collision cell is first filled with the target gas, and counting rates of the fast neutrals (S_o) and the primary ions (S_q) is measured with and without the deflection field*. The cell is then evacuated, and the same procedure is repeated. The fast neutral signals are corrected with those with the empty cell. Attenuation of the primary ion beam is generally negligible**. Throughout the measurement, the primary ion beam intensity is reduced to the order of 10^4 counts/sec to ensure normal counting efficiency.

The cross section σ_{qo} for the process (3) is given by

$$\sigma_{qo} = \frac{\gamma_q \cdot S_o}{\gamma_o \cdot S_q \cdot N \cdot L} \qquad (4)$$

wher, γ_o and γ_q are the detection efficiencies of the fast neutrals and

---

*,** Since S_o is less than 1 % of S_q except for the case of q=1, contribution from the fast neutrals to S_q can be neglected. The S_q may contain contributions from q-s (s<q) hold charge state of ions produced in the collison cell, but they are neglected also.

the primary ions of the q-th charge state.

Since the experiment is made at the ion acceleration voltage higher than 1 kV, and the ions are accelerated further by the multiplier voltage before hitting the aluminum plate, the detection efficiency of ions, γ_q, may be considered as unity for single particle counting mode. For neutral atoms, the detection efficiency, γ_o, may not necessarily be unity especially when the primary ion energy is low. At the energies above a few keV, however, γ_o may be considered as unity without big errors. Therefore, we simply assume $\gamma_o = \gamma_q = 1$. If the γ_o is smaller than γ_q, the real cross section will be bigger than the measured one.

Fig. 2 shows the cross sections obtained for Ne and Ar. As the measured points are rather scattered, horizontal lines are drawn only for reference of average values. The cross sections σ_{3o} reported by Latypov et al.[2] are shown as a reference. The cross sections σ_{5o} for Ne and Ar are not determined because the primary ions are not separated from the impurity ions; C^{3+}, O^{4+} and O^{2+}.

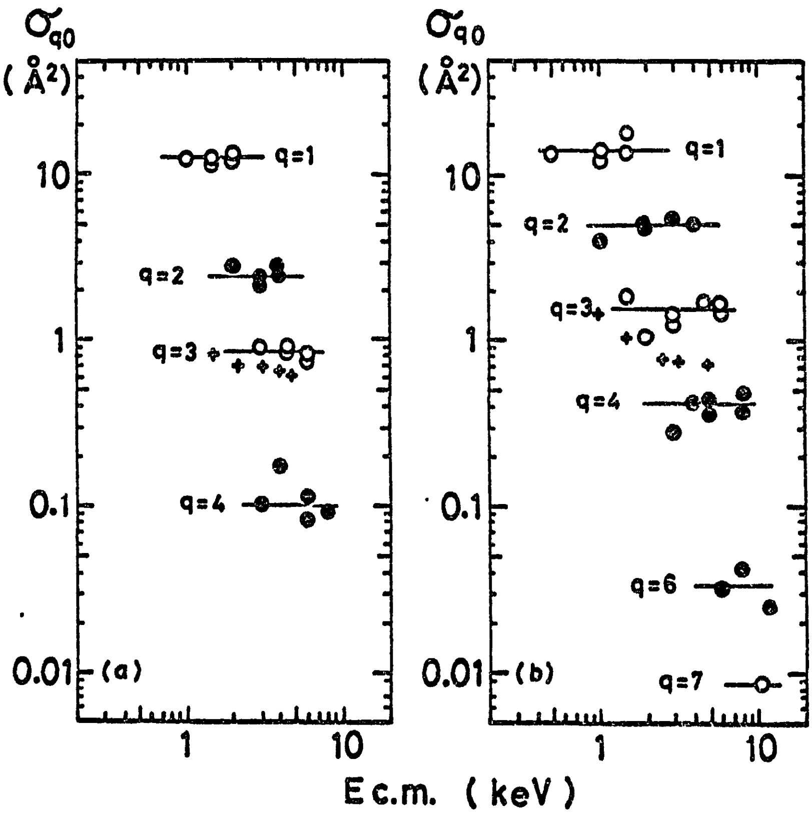

Fig. 2. Cross sections for symmetric resonance multiple charge transfer processes; (a) Ne^{q+}+Ne, (b) Ar^{q+}+Ar.

The obtained cross sections appear to decrease with an increase of the q-value for both cases of Ne and Ar. Such features are clearly seen in Fig. 3, where the mean values of cross sections are plotted against the charge state q at the collision energy around 5 keV. As indicated by

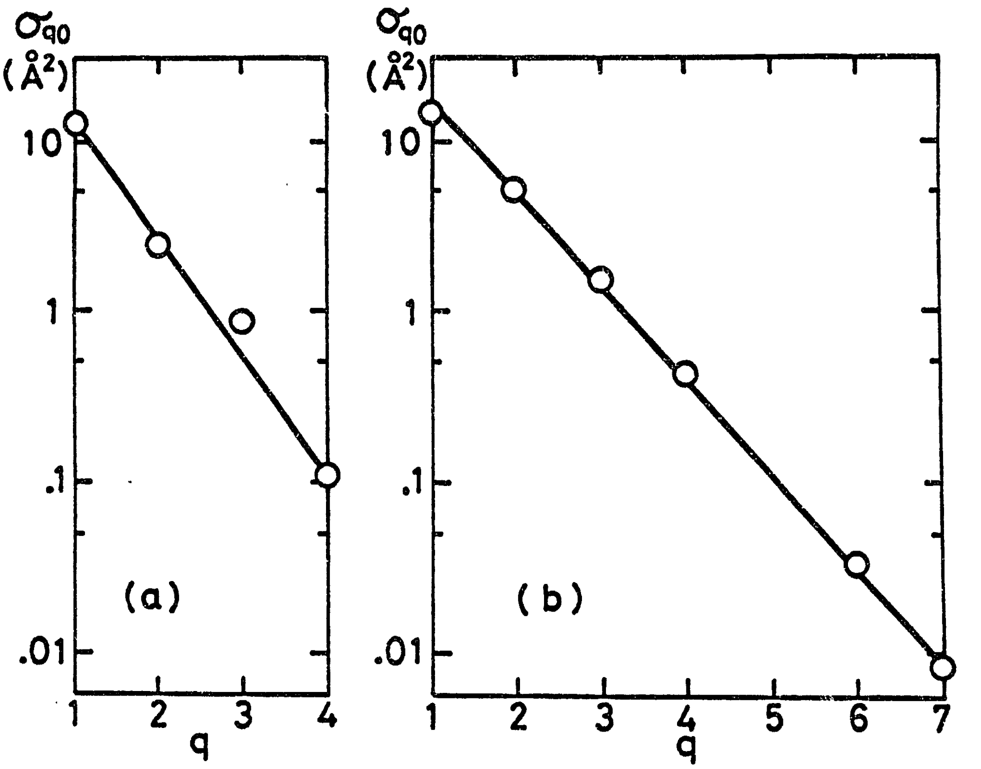

Fig. 3. Cross sections determined at 5 keV for each charge state q; (a) Ne^{q+}+Ne, (b) Ar^{q+}+Ar.

solid lines, the relationship between σ_{qo} and q is approximately expressed by

$$\sigma_{qo} = (5.0)^{-(q-1)}\,\sigma_{1o} \qquad \text{for Ne,} \qquad (5)$$

and

$$\sigma_{qo} = (3.5)^{-(q-1)}\,\sigma_{1o} \qquad \text{for Ar.} \qquad (6)$$

There might be a possibility that the observed signals involve contribution from VUV- or soft-X ray photons emerging from the collision cell. The time-of-flight measurements confirmed that this contribution was two orders of magnitude less than the fast neutral signals.

DISCUSSION

The measurement of cross sections, described in the preceding section is a preliminary one. There might be some sources of errors, which have not yet been checked. Angular distribution of the fast neutrals has not been studied. Energy dependence of the measured cross sections has not been clear because of the scattering of the measured points. Therefore, the accuracy of the measured cross sections can not be insisted to be so high. Especially, for the highest charge states in the both Ne and Ar cases, the measured cross sections may have errors of factor of two. However, it can not be denied that resonance charge transfer really occurs for $q \leq 4$ (Ne), and for $q \leq 7$ (Ar) at several keV collisions. It is exciting to imagine that seven electrons jump together from an atom to an ion.

Okuno et al.[3] measured the cross sections of symmetric resonance charge transfer of single and double charged ions for Kr and Xe in the energy range from the room temperature to 20 eV by the injected-ion drift tube technique. The results are shown in Fig. 4. The cross sections for double charge transfer increase steeply with the decrease of energy below 1 eV, and fit well on the classical orbiting cross sections multiplied by a factor of 1/2. Their conclusions are summerized as follows;

(1) A probability for resonance double charge transfer is 1/2.

(2) $\dfrac{\sigma_{2o}}{\sigma_{1o}} \simeq \dfrac{I_1}{I_1 + I_2}$ above 1 eV, where I_1 and I_2 are the first and second ionization potentials, respectively.

(3) $\sigma_{2o} > \sigma_{1o}$ at the room temperature.

Okuno et al.[4] measured cross sections of similar process for Kr^{3+} in a few keV region, and found that tripple charge transfer has also a fairly large cross section. These experiments were what stimulated us to perform the present work.

In the Rapp-Francis theory for symmetric resonance single charge transfer,[5] which takes only u-g interaction into account, the cross section is approximately given by

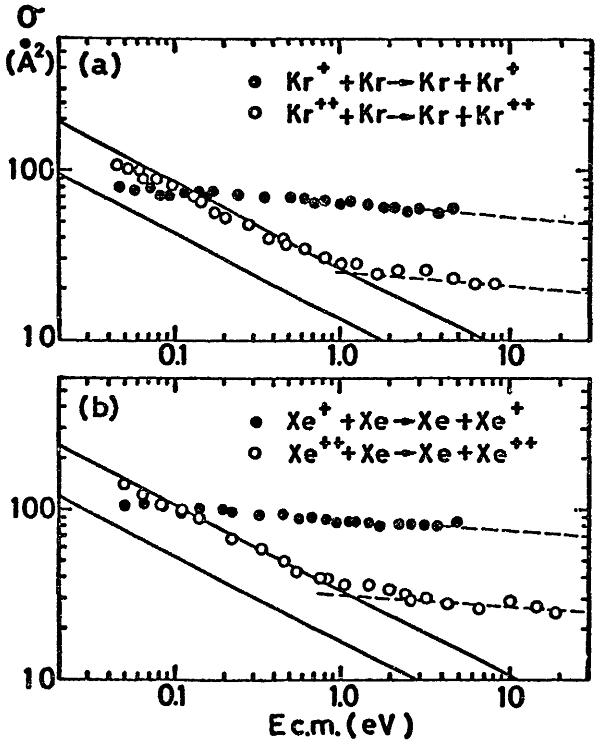

Fig. 4. Cross sections of single and double charge transfer for Kr and Xe by injected-ion drift tube technique[3].

$$\sigma(v) = \frac{1}{2}\pi\, r_c(v)^2, \qquad (7)$$

where $r_c(v)$ is the nuclear distance at which the u-g oscillation nearly ends during the collision. At a fixed velocity, r_c is considered as a sort of collision diamerer, since a resonance charge transfer process is an inversion of elastic scattering.

For a crude discussion, let us extend this idea to the symmetric resonance multiple charge transfer processes. Then we find that the r_c given by eq.(7) is very small even though the cross section σ_{qo} appears fairly large. For example, r_c will be 1×10^{-9} cm for $\sigma_{7o}(Ar)$, which is much smaller than the size of an atom. This means the two state approximation is false for multiple charge transfer. We must take other competing channels into account. Fig. 5 shows schematic diagrams of potential curves for Ar^{2+}-Ar and Ar^{3+}-Ar systems. In the case of Ar^{2+}-Ar, no potential curve crosses the curve for initial state at a larger distance than r_c. In contrast to that, in the case of Ar^{3+}-Ar, a number of potential curves for Ar^{2+*}-Ar^{+} cross the potential curve of the initial state at the outside of r_c. In fact, it is well known that one electron capture process has a large cross section around 1 x 10^{-14} cm^2 for highly charged ions[6]. This suggests that competition with other channels is what makes apparent probabilities of resonance multiple charge transfer small.

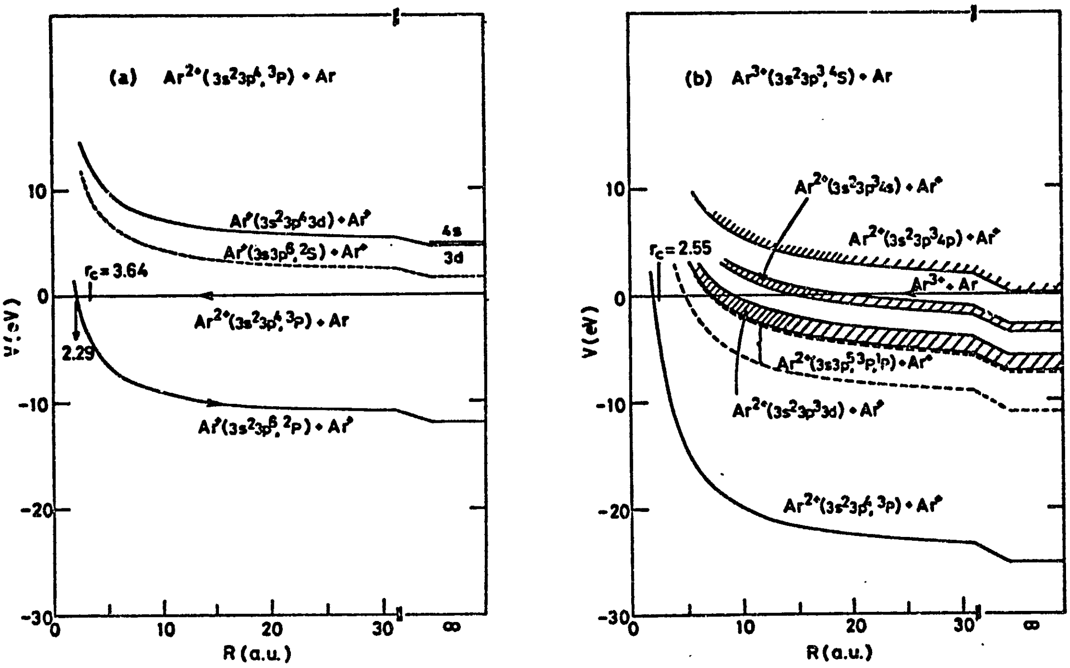

Fig. 5. Schematic diagrams of potential curves; (a) Ar^{2+}+Ar, (b) Ar^{3+}+Ar.

Thus, it is most interesting what will happen to the resonance multiple charge transfer in a very low energy. The classical orbiting cross section is larger for higher charge state of ions, of course. If the probabilities of one electron capture processes decrease in a very low energy, resonance multiple charge transfer may have a very large cross section. If this could happen, it would affect the energy distribution of highly charged ions in a low T_i (but high T_e) plasma.

The author is grateful to Professor K. Takayama, the Director of IPP, for his encouragement through this work.

REFERENCES

1) E. D. Donets, Sov. Bul. "Disc. Invent.", No.24 (1967), and E. D. Donets, IEEE NS-23, 897 (1976)

2) Z. Z. Latypov, N. V. Fedrenko, I. P. Flaks and A. A. Shaporenko, Sov. Phys. JETP 28, 439 (1969)

3) K. Okuno, T. Koizumi and Y. Kaneko, Phys. Rev. Letters 40, 1709 (1978)

4) K. Okuno, T. Koizumi and Y. Kaneko, Book of abstracts of X-ICPEAC, Kyoto (1979) p.594

5) D. Rapp and W. E. Francis, J. Chem. Phys. 37, 2631 (1962)

6) H. Klinger, A. Müller and E. Salzborn, J. Phys. B 8, 230 (1975)

IMPURITY RADIATION LOSSES IN FUSION PLASMAS

D. E. Post*
Plasma Physics Laboratory, Princeton University
Princeton, New Jersey 08544 USA

This paper will stress the viewpoint of radiation as an energy loss channel for fusion plasmas in general, and tokamaks, in particular. It will address atomic physics from a consumer point of view, and discuss how one might model radiation losses from fusion plasma experiments using the best available data. The paper is aimed primarily at the atomic physicist who wishes an introduction to how his work impacts fusion. The paper will begin by discussing what conditions (n_e, T_e, etc.) characterize fusion plasmas. A brief history of the relevant atomic physics calculations will be described and the relevant atomic processes outlined. The implications of these calculations and the effects of impurity radiation in tokamak experiments will be discussed, followed by a capitulation of new work and a summary.

Fusion plasmas require fusion, usually DT fusion. This requires an ion temperature on the order of 10 keV. A second requirement is that β (the ratio of the plasma pressure to the magnetic pressure) be of the order 10% - 100%, and that the plasma be close to ignition where the alpha heating power is sufficient to compensate the losses ($n_e\tau_e \sim 10^{14}$ sec cm^{-3}). This means that such plasmas have 10^{12}cm^{-3} < n_e < 10^{16}cm^{-3} keV $\lesssim T_e \lesssim 5 \times 10^4$ eV, and 10^{-3} sec < $\tau_e \sim 1$ sec or longer. There are parameters which allow us to neglect photo-ionization, radiative transfer calculations, and assume that all excited ions decay to the ground state without interference.

Impurities have two primary harmful effects. The first is that they lose energy by line radiation and bremsstrahlung. The second is that they contribute extra electrons, which dilute the reacting hydrogen (assuming that the plasma pressure is fixed). High Z impurities are worse than low Z because they have more electrons and require higher electron temperatures to strip out to the nonradiative He-like state. A third effect is that they can radiate energy from the edge, thereby spreading the plasma heat load out uniformly on the wall.

Present tokamaks lose energy from the center by high Z radiation and conduction. They lose energy from the edge by ionization, low Z radiation, and charge exchange.

Early calculations of impurity radiation (such as R. F. Post)[1] considered only systems with a few electrons, but recognized the importance of nonequilibrium effects. Hinnov[2] (1970), using radiative recombination, suggested a useful rule of thumb $P_z \sim N_e N_z \, 10^{-26}$ watts/cm^3. Cox and Tucker[3] (1969) published cooling rate curves for elements from He to S which included dielectronic recombination. In 1975 they were followed by Merts, et al.[4] who calculated iron. In 1976 results appeared on molybdenum[5,6] and tungsten[6]. In 1976 Cowan[7] at LASL calculated spectra for tungsten, which allowed the spectroscopic identification of tungsten light in tokamaks for the first time.[8]

Power loss calculations have different requirements than spectroscopy. First, one must determine the distribution of ionic states from recombination and ionization rates. Then, one must determine the radiation from each state. One needs a complete set of rates for all ionic species, so broad, general, formulae and presecriptions are needed. These rules are calibrated by comparison with detailed results for a few species at a few data points.

As an illustration of the kinds of rates used in modeling, we shall outline the rates used in the Princeton code.[9] Collisional ionization is calculated using modifications of Lotz.[10] Recombination includes radiative rates (Seaton[11] plus others), three body rates, dielectronic rates (Burgess[12] plus Merts[4]), and, in some cases, charge transfer (from neutral hydrogen) rates. Collisional excitation largely follows prescriptions of Seaton.[11] The average ion model described in Ref. 9 has been replaced by a treatment of each species.

A coronal equilibrium calculation with these rates is given in Fig. 1. The key new feature as dielectronic recombination, which increases the radiation at 1 - 2 keV by reducing the average charge from 48 to 33.

The effect of this radiation can be estimated for fusion reactors by balancing the alpha heating with radiation losses and transport losses. Defining the critical impurity concentration as the level at which the alpha heating equals the radiative cooling, one finds that very small amounts ($\sim 10^{-4}$) of tungsten can prevent ignition.[13]

Early fusion experiments (1955 - 65) had difficulty "burning out" low Z (C, O) impurities ($T_e \sim 20$ eV). This problem was solved by tokamaks in the USSR by the use of metal limiters to keep the plasma away from the wall, "discharge cleaning," and heating with a large plasma current. Once temperatures greater than 100 eV were obtained the losses were by conduction, convection, and charge exchange. As the size of experiments increased, the plasma losses were reduced since they are diffusive and thus drop proportional to $1/a^2$. Volume losses such as impurity radiation became important again, especially with advent of high power heating with neutral beams which led to high power densities on limiters. On ORMAK,[8] PLT,[14] DITE,[15] and TFR,[16] radiation from tungsten and molybdenum was responsible for much of the energy losses. On PLT tungsten radiation caused hollow T_e profiles, and neutral injection served only to increase the tungsten radiation. The tungsten limiter was replaced by a carbon one, and record temperatures were obtained.[17]

Impurities were also thought to be effective in stopping the penetration of high energy neutral beams.[18] Recent results[19] have shown that there is very little effect primarily due to the fact that charge transfer is more likely than ionization. This, however, means that charge transfer between highly ionized impurities and neutral hydrogen can be an important recombination mechanism. This charge transfer recombination rate is typically greater than the radiative recombination rates, and less than dielectronic rates, so it is important, primarily, for the fully stripped to carbon-like states. For a fixed neutral fraction, $f_o = n_o/n_e$, the relative abundance of ionic states and radiation rates are independent of n_e. Charge exchange recombination can enhance iron radiation by factors of 10, and never allow the stripping out of Fe even at $T_e = 100$ keV. Experimental evidence has been quoted for oxygen (Isler[20]) and results from PLT (Post[21]) show some justification that it may exist. The Fe XXIV light rises dramatically (x 30) with 2 MW of injection into a plasma with T_e = 2 - 3 keV (Fig. 2). There is some indication that charge exchange recombination (with thermal neutrals as well as beam neutrals) may be responsible for a portion of the disagreement between the measured ionic species distribution and coronal equilibrium. One area for future work in radiation loss (not diagnostics) will be impurity control. We do not understand how impurities enter the plasma, how they are transported, and how they leave the wall. There are three leading candidates for impurity generation: (1) Sputtering of walls, limiter by charge exchange neutrals, (2) sputtering by ions, and (3) arcing. The study of the transport of the impurities will involve multispecies impurity transport codes (e.g., Amano, et al.[22]). There is some interest in enhancing low Z radiation to keep the edge cool, reducing the power incident on the limiter.[23] Charge exchange recombination will continue to be of interest. There is diminished interest in high Z atomic physics, since high Z elements can be kept out of experiments. There will continue to be interest in good rates, etc., for diagnostic purposes.

The success of fusion depends not only on controlling and minimizing plasma transport losses, but also minimizing and controlling central impurity radiation losses. One of the major advances in the last three years in fusion has been the identification of high levels of radiation from high Z materials, and their removal from experiments. Future tokamak experiments plan to use low Z limiters and/or divertors PDX, JT-60, TFTR, INTOR for impurity control. Promising new directions for research are charge exchange recombination, the physics of impurity generation, impurity transport, and diagnostics. For all of these, one will need good quality rates for low and medium z elements. We shall end by remarking that impurity radiation problems are a measure of the success of tokamaks. As other devices solve the plasma physics problems and reduce plasma energy and particle losses, they will encounter impurity problems, and must solve them also.

ACKNOWLEDGMENTS

This work was supported by United States Department of Energy Contract No. EY-76-C-02-3073.

REFERENCES

1. R. F. Post, J. Nucl. Energy C3 (1961) 273.

2. E. Hinnov, MATT-777 (1970), Princeton University Plasma Physics Laboratory, Princeton, NJ 08544.

3. D. Cox and W. Tucker, Astrophys. J. 157, 1157 (1969).

4. A. L. Merts, R. D. Cowan, and N. H. Magee, Jr., LASL Report, LA-6220-MS, Los Alamos, NM (1976).

5. C. Breton, C. DeMichelis, and M. Mattioli, EUR-CEA-FC-853 (1976).

6. R. V. Jensen, D. E. Post, W. H. Grasberger, C. B. Tarter, and W. A. Lokke, Nucl. Fusion 17, 1187 (1977).

7. R. D. Cowan, LA-6679-MS, Los Alamos National Laboratory, Los Alamos, NM (1977).

8. R. C. Isler, R. V. Neidigh, and R. D. Cowan, Phys. Lett. A 63A, 795 (1977).

9. D. E. Post, R. V. Jensen, C. B. Tarter, W. H. Grasberger, and W. A. Lokke, Atomic Data and Nucl. Data Tables 20, 397 (1977).

10. W. Lotz, Astrophys. J. Suppl. 14, 207 (1967).

11. M. Seaton, Mon. Not. R. Astron. Soc. 119, 81 (1959); also "The Theory of Excitation and Ionization by Electron Impact" in Atomic and Molecular Processes, ed. D. R. Botes, (Academic Press, Inc., New York, 1962).

12. A. Burgess, Astrophys. J. 141, 1588 (1965).

13. R. V. Jensen, D. E. Post, and D. L. Jassby, Nucl. Sci. Eng. 65, 282 (1978).

14. K. Bol, et al. (PLT Group), IAEA-CN-37/A-1, Innsbruck, (1978), Nucl. Fusion Suppl. 1, (1979), 11.

15. N. Peacock, et al. (DITE Group) IAEA-CN-37/N-5/2, Innsbruck, (1978), Nucl. Fusion Suppl. 1, (1979), 303.

16. Equipe TFR, Nucl. Fusion 18, (1978), 791.

17. H. Eubank, et al. (PLT Group), IAEA-CN-37/C-3, Innsbruck, Nucl. Fusion Suppl. 1, (1979), 167.

18. J. Girard, D. A. Martz, P. Moriette, Proc. V Int. Conf. Plasma Phys. and Contr. Nucl. Fusion Res., V. 1, (1974), 681.

19. R. E. Olson, et al., Phys. Rev. Lett. 41, (1978), 163.

20. R. C. Isler and E. C. Crume, Phys. Rev. Lett. 41 (1978), 1296.

21. D. E. Post, R. A. Hulse, E. Hinnov, and S. Suchewer, XI ICPEAC, Kyoto, Japan (1979) 4I13.

22. M. Ohamoto and T. Amano, J. Comp. Phys. 26, (1978), 80.

23. S. Suckewer and R. J. Hawryluk, Phys. Rev. Lett. 40, (1978), 1649.

FIGURE CAPTIONS

Fig. 1. Power radiated per free electron per ion in coronal equilibrium for a number of representative elements.

Fig. 2. The Fe XXIV light in a 2.1 MW PLT neutral bean injection experiment. The beam is on from 450 ms to 600 ms. (E. Hinnov)

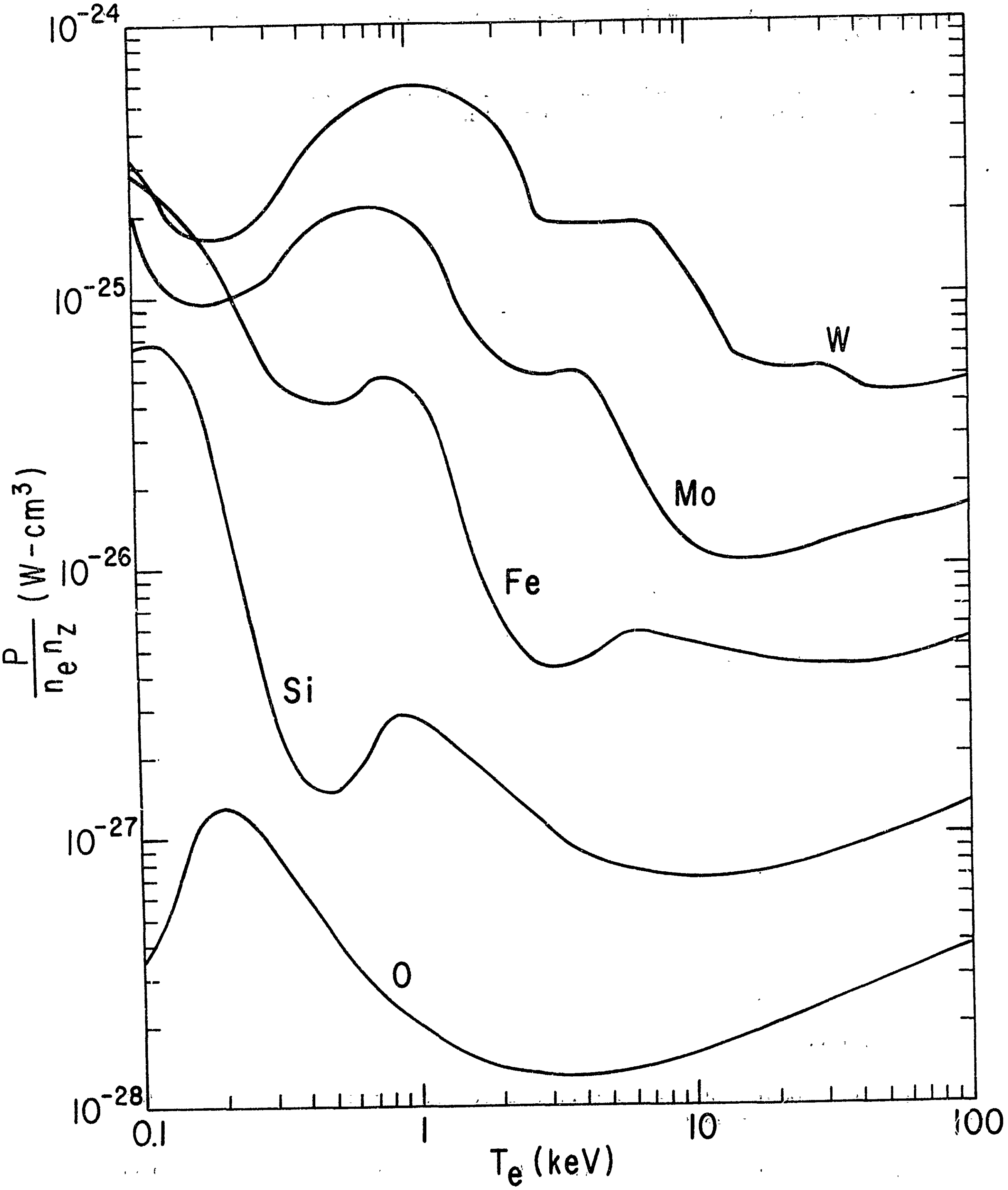

10^{-24}
10^{-25}
10^{-26}
10^{-27}
10^{-28}
$\frac{P}{n_e n_z}$ (W-cm^3)
W
Mo
Fe
Si
O
0.1
1
10
100
T_e (keV)

Fig. 1

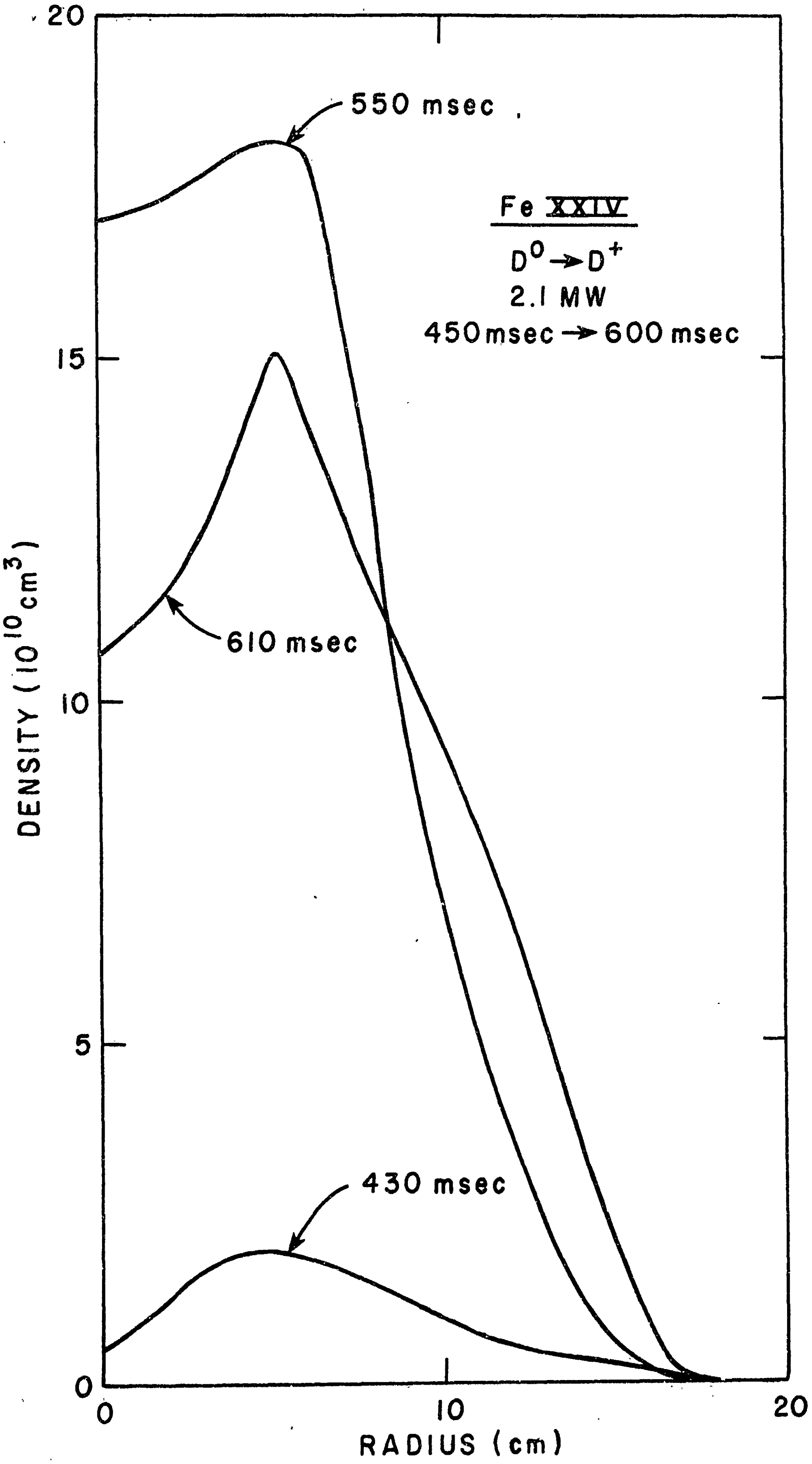

20
15
10
5
0
DENSITY (10^{10} cm^3)
550 msec
610 msec
430 msec
Fe XXIV
$D^0 \rightarrow D^+$
2.1 MW
450 msec → 600 msec
0
10
20
RADIUS (cm)

Fig. 2

ATOMIC COLLISIONS IN FUSION PLASMAS INVOLVING MULTIPLY CHARGED IONS

E.Salzborn

Institut für Kernphysik, Universität Giessen, D-6300 Giessen, W.-Germany

ABSTRACT: A short survey is given on atomic collisions involving multiply charged ions. The basic features of charge transfer processes in ion-ion and ion-atom collisions relevant to fusion plasmas are discussed.

INTRODUCTION

The properties and operation of thermonuclear fusion plasmas are significantly affected by the presence of highly charged impurity ions. Not only that the impurities have a large influence on important plasma parameters like power balance, temperature, resistivity, and stability; but also, being present in quantities above critical concentrations, they even prevent achieving energy break-even[1,2]. Thus, the physical processes involving impurities are of basic interest for confined plasma research. The needs are to understand the release of impurities by plasma-surface interaction, their collisional interactions with the plasma constituents, the plasma energy loss by radiation cooling, and last but not least it is vital to find methods to reduce the impurity concentrations below tolerable levels.

In fusion plasmas impurities inevitably occur. Stainless steel being widely used for Tokamak vacuum vessels is an almost inexhaustible supply of C and O unless coated or carefully treated. From the walls or other structure materials (e.g.limiters) additionally atoms for example of Ti, Cr, Mn, Fe, Ni, Mo or W are released by sputtering, desorption or blistering. In present-day fusion devices concentrations in the order of 0.5-5 % oxygen, 0.1-0.5 % iron and $\simeq$ 0.1 % molybdenum or tungsten have been detected by optical spectroscopy.

The impurities diffusing from the wall into the plasma are successively ionized by electron impact yielding ions in increasing charge states. In the plasma center low Z elements like C and O are completely stripped, higher Z impurities attain very high charge states, e.g.Fe^{24+} or Mo^{34+}.

The present paper shortly reviews collision processes in fusion plasmas involving multiply charged ions. Not considered are electron-ion collisions which are discussed in another contribution to this conference.

COLLISIONS INVOLVING MULTIPLY CHARGED IONS

I) ION - ION COLLISIONS

The simplest multiply charged ion, the generation of which is being ardently longed for in fusion plasmas, is the He^{++} ion resulting from the fusion reaction itself:

$$d + t \rightarrow He^{++}(3.5\ \mathrm{MeV}) + n(14.1\ \mathrm{MeV}) \qquad (1)$$

The He^{++} ions, released at 3.5 MeV kinetic energy and confined by the toroidal magnetic field, are to maintain the plasma temperature by Coulomb collisions with the plasma constituents. Nevertheless, from a plasma physical point of view they have to be considered as impurities which should be removed from the plasma center.

Very recently, Olson[3] has pointed out that the desired α-particle heating of the plasma will be reduced if the He^{++} ions should capture one or even two electrons from partially stripped impurity ions. Applying a classical-trajectory Monte-Carlo method Olson has calculated the capture cross sections $\sigma_{2,1}$ for He^{++} ions colliding with oxygen ions. The results for He^{++} impact energies between 1 and 2 MeV on O^{3+} and O^{5+} ions are shown in Fig.1.

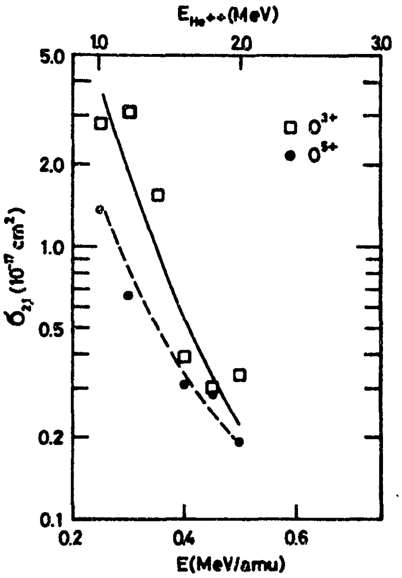

Fig.1:
Calculated one-electron capture cross sections $\sigma_{2,1}$ for He^{++} ions colliding with O^{3+} (□) respectively O^{5+} (•) ions. Lines are drawn through the theoretical points as a visual aid.

The cross sections increase in this range with decreasing impact energy from approximately $2 \cdot 10^{-18}$ cm^2 to some 10^{-17} cm^2. At a 0.1% oxygen charge state concentration corresponding to about 10^{11} impurity ions/cm^3 in a Tokamak plasma a collision period for electron capture of $5 \cdot 10^{-3}$ s to $7 \cdot 10^{-4}$ s results which is shorter than the α-particle heating period of $\approx$ 0.1 s. Although the resulting He^{+} ion will be reionized to He^{++} by collisions with electrons or deuterons within 10^{-6} s (at densities of $n_e = n_d = 10^{14}$ cm^{-3}) the orbit along the corresponding travel distance of about 10 m is distorted which might cause a loss from the plasma. A loss of α-particle heating definitely will occur in the case of double electron capture by He^{++} to He. Fortunately however, the corresponding cross sections σ_{20} are about two orders of magnitude smaller than $\sigma_{2,1}$. Thus, depending on the concentration and charge state distribution of impurity ions across the plasma radius there may be a loss of α-particle heating efficiency due to electron capture in He^{++} - impurity ion collisions.

There is no experimental data to compare the cross sections predicted by Olson with. Because of the extreme difficulties involved in the measurement not a single experiment studying electron capture cross sections in collisions between two multiply charged ions has been published. The only work reporting charge transfer cross sections for ion-ion collisions has recently been performed[4] with singly charged ions, namely H^+ incident on He^+.

II) ION - ATOM COLLISIONS

1) COLLISIONS INVOLVING HYDROGEN ATOMS

Inspite of the high temperature there is a small but finite concentration of neutral hydrogen even in the plasma center due to electron-ion recombination. The neutral density n_o decreases between wall and plasma center over about two orders of magnitude yielding a ratio of approximately $n_o/n_e \cong 10^{-5}$ on the axis of present-day Tokamaks. In future devices like the TFTR values of $n_o/n_e \cong 10^{-8}$ are expected[5].

During the last years much effort has been spent, both theoretical and experimental, to investigate charge transfer between highly charged ions and atomic hydrogen. To understand these processes not only is important for the collisions occuring in the plasma itself at energies of a few keV but also for the physics of neutral beam heating involving collisions at several tens of keV. Most theories[6-14] regard to completely stripped ions, most experiments[15-18] however involve only partially stripped ions.

The general features of the electron capture cross sections have become more and more clear now. The theories which fairly close approach experimental data are the method of coupled molecular orbits for the low energy range ($\lesssim$10 keV/amu), a classical-trajectory Morte-Carlo method for the intermediate energy range (10-100 keV/amu) and a unitarized distorted wave approximation (UDWA) for the low, intermediate and high (>100 keV/amu) energy range.

In Fig.2 total capture cross sections calculated by UDWA[19] are compared with experimental data. The cross sections and the impact energy are scaled as $\sigma(E)=\alpha\cdot\tilde{\sigma}(\tilde{E})$ and $E=\beta\cdot\tilde{E}$, respectively, with $\alpha=Z^{1.07}$ and $\beta=Z^{0.464}$ where Z denotes the ionic charge.

In general, the capture cross sections are almost energy independent for scaled impact energies of approximately $\tilde{E}<10$ keV/amu and decrease rapidly above this limit falling on a smooth universal curve for energies $\tilde{E}\gtrsim 100$ keV/amu. These results of Ryufuku and Watanabe[19] are in good agreement with the experimental data below about 100 keV/amu; at higher energies they tend to slightly overestimate the data.

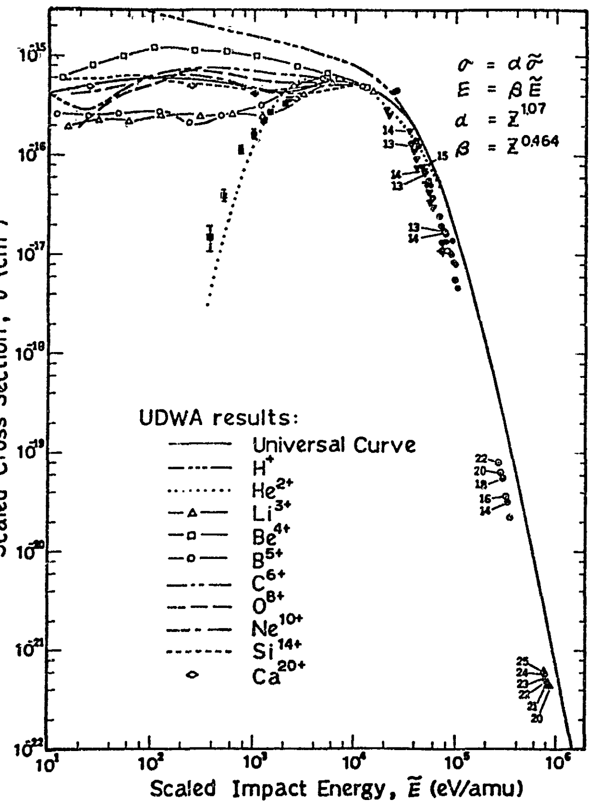

Fig.2:
Calculated scaled total electron capture cross sections $\tilde{\sigma}$ versus scaled impact energy $\tilde{E}$ for collisions of completely stripped ions of charge Z with atomic hydrogen.
Experimental data:
(He^{2+} + H) Nutt et al.[20],
(O^{8+} + H) Meyer et al.[18],
(Ar^{8+} + H) Crandall[17],
($Fe^{(9-13)+}$ + H) Gardner et al.[15],
($Fe^{(9-15)+}$ + H) Meyer et al.[18],
($Fe^{(9-22)+}$ + $0.5H_2$) Berkner et al.[21],
($Fe^{(20-25)+}$ + $0.5H_2$) Berkner et al.[22].
(from Ref.19)

In the impact energy range E>50 keV/amu another scaling approach has been given by Chan and Eichler[14]. These authors show that the total capture cross sections can be expressed by

$$\sigma = \alpha(Z,v) \cdot \sigma^{OBK}(Z,v) \qquad (2)$$

with $\sigma^{OBK}(Z,v)$ denoting the well known Oppenheimer-Brinkman-Kramers[23] cross sections summed over all principal shells and $\alpha(Z,v)$ being a scaling factor which is almost independent of the ionic charge Z.

The knowledge of these cross sections over a large energy range is of particular importance for the neutral beam injection into fusion plasmas which until now is by far the most successful heating method. Very recently, in Princeton[24] injection of 2.4 MW of 40 keV D^o increased the H^+ ion temperature by a factor of six up to 6.5 keV. For the penetration into the center of future ignition-sized Tokamak plasmas however much higher neutral beam energies in the range above 200 keV D^o are estimated[25].

With increasing energy the trapping of the injected neutral beam by impact ionization on plasma ions becomes dominant over trapping by charge exchange and electron ionization. In order to predict the penetration and energy deposition, therefore also cross sections for impact ionization by highly charged ions via the reaction

$$H^o + A^{Z+} \rightarrow H^+ + e + A^{Z+} \qquad (3)$$

have to be known. Especially Olson and Salop[8] have investigated this problem in detail by classical-trajectory Monte-Carlo calculations. In Fig.3 theoretical impact ionization cross sections for fully stripped A^{Z+} ions colliding with H atoms are shown. The cross sections peak at higher energies as Z increases from H^+ up to Kr^{36+}. Thus, the energy dependence is different from that predicted by the binary encounter approximation[26] from which the cross sections scale as Z^2 times the $H^o + H^+$ results.

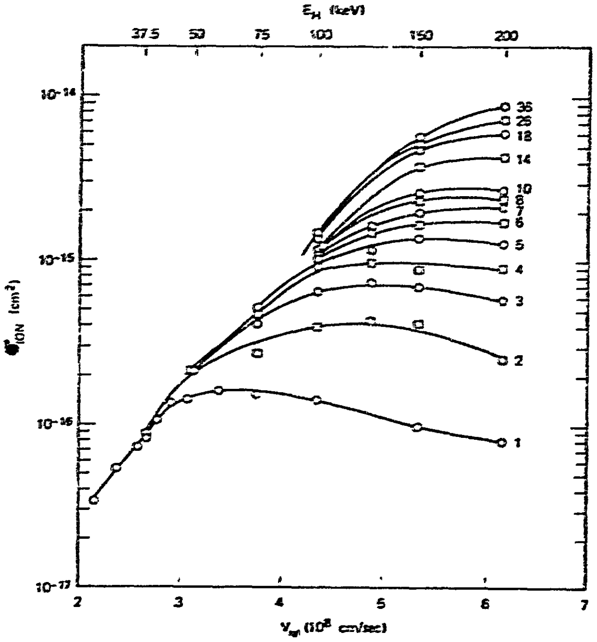

Fig.3:
Calculated impact ionization cross sections σ_{ion} for fully stripped ions of charge $1 \leq Z \leq 36$ colliding with H atoms (from Ref.8).

The corresponding total electron capture cross sections for the reaction

$$H^o + A^{Z+} \rightarrow H^+ + A^{(Z-1)+} \qquad (4)$$

calculated by applying the same theory[8] are presented in Fig.4. The curves show a progressively weaker energy dependence as the charge Z increases from 1+ up to 36+. Again, note that a simple Z^2 scaling of the $H^o + H^+$ cross section would reproduce neither the shape nor the magnitude of these cross sections.

The sum of impact ionization (Fig.3) and electron capture (Fig.4) cross sections which determines the additional attenuation and reduction of penetration length of the injected energetic neutrals by fully stripped impurity ions is shown in Fig.5. These cross sections are for the higher Z values almost constant in the energy range 40 keV$\leq E_H \leq$200 keV. At a collision energy of E_H=50 keV which is close to present-day neutral beam injection energies the sum of both cross sections $\sigma_{loss} = \sigma_{ion} + \sigma_{cex}$ approximately scales as

$\sigma_{loss} \simeq 2.5 \cdot 10^{-16} \cdot Z^{1.25}$ cm^2.

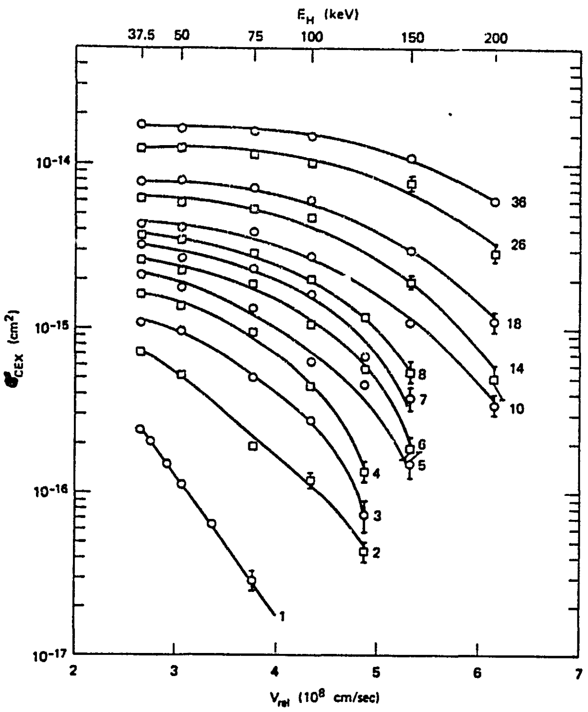

Fig.4:
Calculated total electron capture cross sections σ_{cex} for fully stripped ions of charge $1 \leq Z \leq 36$ colliding with H atoms (from Ref.8)

Unfortunately, experimental data to compare the calculated cross sections with are available only for the case of electron capture by partially stripped ions of low Z elements. There however the agreement between theory and experiment is fairly good.

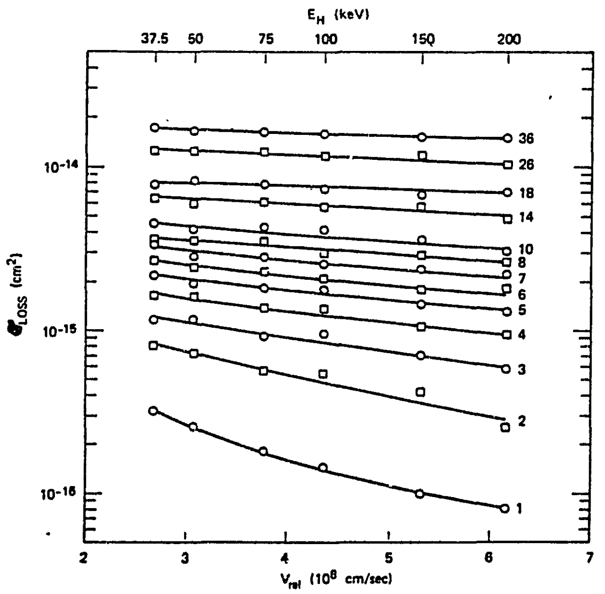

Fig.5:
Calculated total electron loss cross sections $\sigma_{loss} = \sigma_{ion} + \sigma_{cex}$ from H atoms colliding with fully stripped ions of charge $1 \leq Z \leq 36$ (from Ref.8).

2) COLLISIONS INVOLVING MULTI-ELECTRON ATOMS

Collisions between multiply charged ions and neutral multi-electron atoms in fusion plasmas occur at most in the wall zone or result from injected neutralized impurities steming from the ion source for neutral beam injection. The relevant impact energies are again in the few keV respectively several tens of keV energy range.

Because of the many electrons involved in these collisions theoretical calculations of charge transfer cross sections are more complicated than in the case of fully stripped ions colliding with atomic hydrogen. Nevertheless, in recent years several theoretical approaches[7,27-29] have been developed which reasonably describe the available experimental data.

The main features of the total electron capture cross sections for collisions between multiply charged ions and multi-electron atoms at impact velocities $v<v_o = 2.2\cdot10^8$ cm/s are as follows[30]:

a) In general, the cross sections for capture of one or several electrons are almost independent of impact energy in the range E<25 keV/amu mentioned.
b) The cross sections generally decrease with the number of electrons transferred in a single ion-atom encounter.
c) The cross sections generally increase with the initial ion charge state i.
d) The cross sections decrease with increasing target ionization potential I_B.

As an example for the points a), b) and c) Fig.6 shows total cross sections $\sigma_{i,f}$ for the capture of up to 4 electrons in single collisions of Xe^{i+} ions (i=2,.....,8) with Kr atoms as a function of the ion velocity. The initial and final charge states of the projectile ions are denoted by (i,f). Some of the cross sections $\sigma_{i,f}$ are connected by lines in order to visualize the weak energy dependence. The latter can be understood by the involvment of a lot of excited states of the resulting ion which are populated by the charge transfer process. The partial cross sections for each specific transition terminating in an excited state may have an individual energy dependence. The total cross section, however, made up by the sum over the involved partial cross sections with maxima at different ion velocities only shows a faded velocity dependence.

During the last years we have systematically investigated electron transfer in various multiply charged ion-atom collision systems at keV impact energies[30-35]. The large amount of experimental data allowed for the extraction of simple empirical scaling rules[36] stating that the capture cross sections $\sigma_{i,i-k}$ (k=number of electrons transferred in a single collision) depend on only two quantities, namely the initial ion charge state i and the ionization potential I_B of the neutral collision partner. Thus, the measured data for all collision systems investigated can be represented by a simple scaling formula

$$\sigma_{i,i-k} = A_k \cdot i^{\alpha_k} \cdot I_{B\,[eV]}^{\beta_k} \tag{5}$$

with the parameters A_k, α_k and β_k being adjusted by a least squares fit.

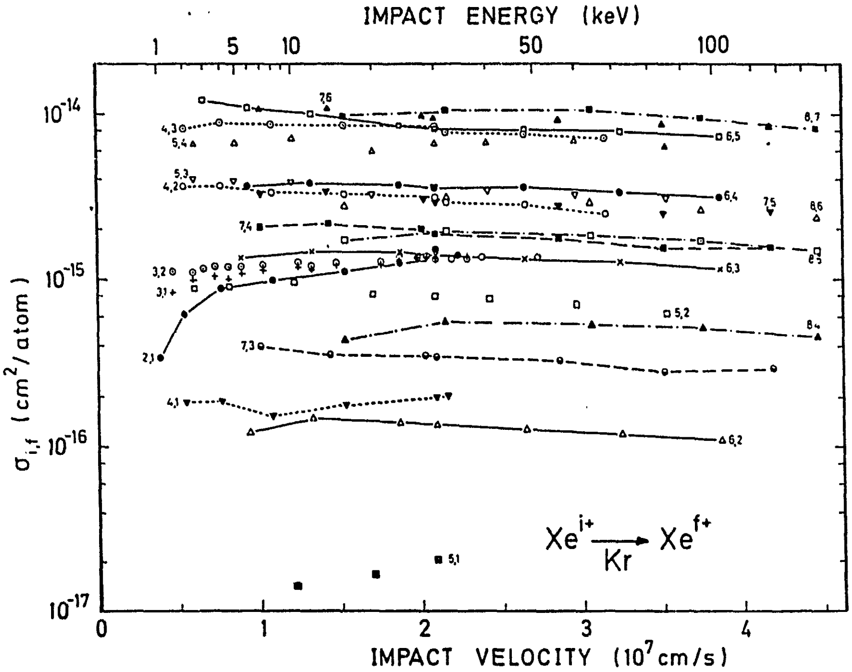

Fig.6: Electron capture cross sections $\sigma_{i,f}$ for Xe^{i+} ions colliding with krypton atoms versus impact velocity[30]. The initial and final charge states are denoted by i and f, respectively. Lines are drawn only as a visual aid.

For example for the capture of one electron (k=1) we have obtained the best fit parameters $A_1=1.43\cdot10^{-12}$ cm^2, $\alpha_1=1.17$ and $\beta_1= -2.76$. These values are based on 107 cross section data for multiply charged rare gas ions ($i\leq8$) colliding with the rare gases He, Ne, Ar, Kr, Xe and the molecular gases H_2, N_2, O_2, CO_2 and CH_4. Within a ±35% margin of error two third of all experimental cross sections are correctly represented by eq.(5). In Fig.7 scaled one-electron capture cross sections for various projectile-target combinations are shown as a function of the initial ion charge state i. The solid line represents eq.(5) with the parameters given above. The empirically obtained power function $\sigma_{i,i-1} \sim i^{1.17}$ is in fairly good agreement with the predicted linear dependence $\sigma_{i,i-1} \sim i$ of Olson and Salop[7], and Grozdanov and Janev[29], respectively. For charge states $i\gtrsim10$, Chibisov[28] predicts $\sigma_{i,i-1} \sim i\cdot\ln i$ and according to Presnyakov and Ulantsev[27] a quadratic dependence $\sigma_{i,i-1} \sim i^2$ is expected.

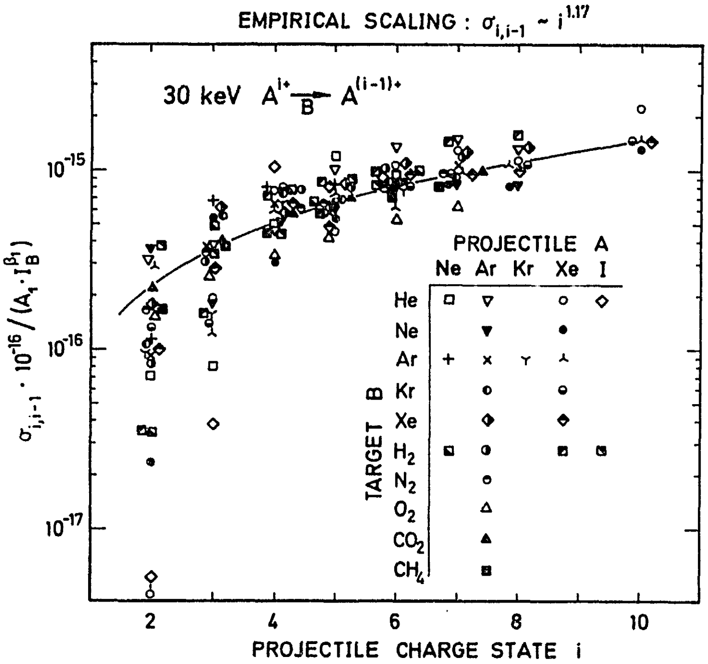

Fig.7: Scaled one-electron capture cross sections for various projectile-target combinations at 30 keV impact energy. The solid line represents the empirical scaling eq.(5).

The second main factor which determines the magnitude of the electron capture cross sections is the ionization potential I_B of the target particle B (see point d). The exponent $\beta_1 = -2.76$ empirically obtained for targets with $I_B \geq 12$ eV is higher than those theoretically predicted which range between $1 \leq \beta_1 \leq 2$. Because of this discrepancy we have extended our experiments to metal vapours with low ionization potentials[37]. The results for 100 keV Xe^{10+} ions incident on target atoms with ionization potentials ranging from $I_B = 3.89$ eV for Cs up to $I_B = 24.58$ eV for He are shown in Fig.8 together with theoretical predictions. The present experimental data are fitted best by a function

$$\sigma_{10,9} = 2.02 \cdot 10^{-12}\ \mathrm{cm}^2 \cdot (I_B/\mathrm{eV})^{-1.94}$$

which is shown by the solid line. Therefore, involving the maximum range of available atomic target ionization potentials an overall cross section dependence close to the inverse square of I_B is observed rather than the stronger dependence based on data for $I_B \geq 12$ eV.

In conclusion, it can be stated that the cross sections for the transfer of electrons in collisions between multiply-charged ions and multi-electron atoms at low velocities ($v < v_0$) show simple features which are reasonably described by generalized theories and by empirical scaling approaches. However, the empirical scaling is based on data involving only low charge states ($i \leq 10$), whereas the relevant theories for one-electron capture are expected to be valid only above lower limits for i ranging from $i \geq 4$ up to $i \geq 10$. Unfortunately, apart from a single estimate[27] for double-electron capture there are no theories available treating multi-electron transfer. This lack is the more pressing since the experiments show that with increasing ion charge state multi-electron transfer becomes more and more likely. It is an open question which processes dominate in collisions between the very highly charged ions occuring in fusion plasmas and multi-electron atoms.

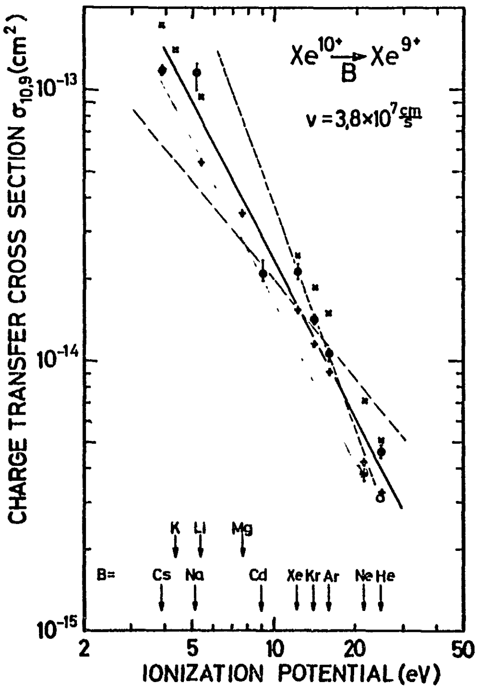

Fig.8:
Cross sections $\sigma_{10,9}$ for one-electron capture by 100 keV Xe^{10+} ions from various target atoms B as a function of the target ionization potential I_B. ● Müller et al.[37] (the targets B used are indicated by the lower row of elements B); —— least squares fit of the experimental data points with a power function of I_B; --- scaling law eq.(5); ... theory of Presnyakov and Ulantsev[27]; ✖ theory of Grozdanov and Janev[29]; ✚ theory of Chibisov[28]; o classical trajectory Monte-Carlo calculation of Olson[38]; -·-·- absorbing sphere model of Olson and Salop[7].

3) CAPTURE INTO EXCITED STATES

Electrons being captured by multiply charged ions from neutral atoms predominantly terminate in excited states of the resulting daughter ion. For fully stripped ions colliding with atomic hydrogen the partial cross sections σ_{nlm}, where n, l and m are the principal, orbital-angular and magnetic quantum numbers, respectively, have been calculated [19,39]. In Fig.9, for an example, the dependence of the partial cross sections $\sigma_n = \sum_{l,m} \sigma_{nlm}$ for collisions between Ne^{10+} respectively Si^{14+} ions and H(1s) atoms on the principal quantum number n of the final state are shown for collision energies between 5 and 2000 keV/amu. The distribution over n is broadest at 100 keV/amu. With increasing energy the quantum number n_m of the state most probably populated decreases and the distribution becomes increasingly smaller. At low energies, the capture mechanism proceeds via coupled molecular orbits resulting in a distribution which abruptly ends at $n=n_m$.

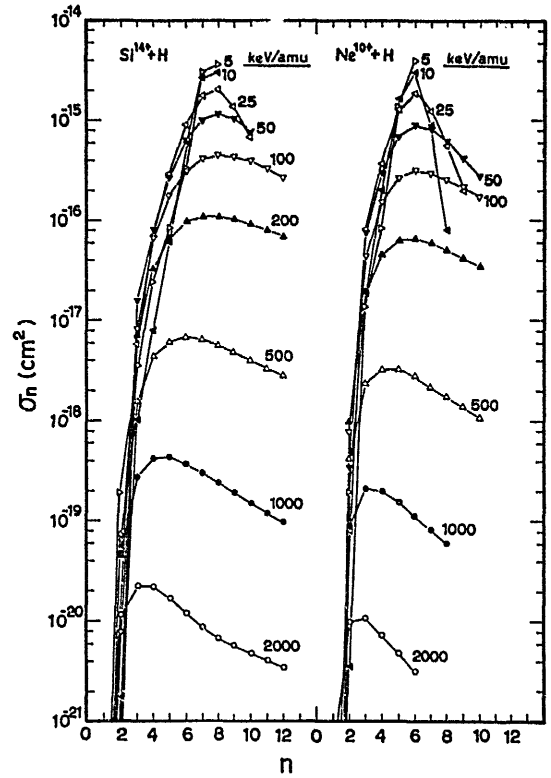

Fig.9:
Partial capture cross sections σ_n for Ne^{10+} + H(1s) and Si^{14+} + H(1s) collisions versus the principal quantum number n of the final state for collision energies between 5 and 2000 keV/amu (from Ref.19).

Experimentally, capture into excited states has been investigated either by detection of the subsequent radiation emission[40,41], by the electron production resulting from radiationless deexcitation of the collision system[42,43], by kinetic energy loss spectroscopy[44] or by a novel recoil method[45]. However, there are no experimental data available to compare the theories of Refs.19 and 39 with.

The emission of radiation subsequent to electron capture into excited states provides an additional energy loss mechanism in fusion plasmas. Indeed, by optical studies of the H^o + O^{i+} collision system at Oak Ridge, this process not only has been observed during the neutral beam injection period[46], but also for noninjected Tokamak discharges[47] where the ambient current densities $n_H \langle v \rangle$ are up to two orders of magnitude smaller. In some circumstances, population of excited states via charge transfer may dominate excitation by electrons. Thus, also for modelling of the plasma impurities charge transfer has to be taken into account as an effective recombination process.

CONCLUSIONS

In recent years, much progress has been achieved towards understanding the basic features of atomic collisions involving multiply-charged ions. Generalized theories as well as empirical scaling rules have been established which reasonably describe experimental charge transfer data. However, for many processes only either calculations or experimental data are available. As to theory there are, for an example, no approaches treating multi-electron transfer. On the other hand, regarding experiments there is, for an example, a lack of data involving highly or even completely stripped ions at low and intermediate impact energies. The latter need can be met if the pulsed electron beam ion sources[48,49] yielding nowadays completely stripped ions of all elements up to argon (Z=18) respectively very high charge states of the heavier elements (e.g. Xe^{44+}) are used also for atomic collision experiments. The answers to these problems are urgently needed for controlled thermonuclear fusion research.

The author wishes to thank his coworker Dr. A. Müller for many stimulating discussions.

REFERENCES

1. D.M.Meade, Nucl.Fusion 14, 289 (1974)
2. H.Vernickel and J.Bohdansky, Nucl.Fusion 18, 1467 (1978)
3. R.E.Olson, Phys.Lett.71A, 341 (1979)
4. G.C.Angel, E.C.Sewell, K.F.Dunn and D.H.Gilbody, J.Phys. B 11, L 297 (1978)
5. J.G.Gilligan, S.L.Gralnick, W.G.Price and T.Kammash, Nucl.Fusion 18, 63 (1978)
6. A. Salop and R.E.Olson, Phys.Rev.A13, 1312 (1976)
7. R.E.Olson and A.Salop, Phys.Rev.A14, 579 (1976)
8. R.E.Olson and A.Salop, Phys.Rev.A16, 531 (1977)
9. J.Vaaben and J.S.Briggs, J.Phys.B 10, L 521 (1977)
10. C.Bottcher, J.Phys.B 10, L 213 (1977)
11. C.Harel an Salin, J.Phys.B 10, 3511 (1977)
12. A.Z.Msezane, Phys.Lett.59A, 435 (1977)
13. H.Ryufuku and T.Watanabe, Phys.Rev.A18, 2005 (1978); A19, 1538 (1979)
14. F.T.Chan and J.Eichler, Phys.Rev.Lett.42, 58 (1979), Phys.Rev.A (to be published)
15. L.D.Gardner, J.E.Bayfield, P.M.Koch, H.J.Kim and P.H.Stelson, Phys.Rev.A16, 1415 (1977)
16. R.A.Phaneuf, F.W.Meyer, R.H.McKnight, Phys.Rev.A17, 534 (1978)
17. D.H.Crandall, R.A.Phaneuf and F.W.Meyer, Phys.Rev.A19, 504 (1979)
18. F.W.Meyer, R.A.Phaneuf, H.J.Kim, P.Hvelplund and P.H.Stelson, Phys.Rev.A19, 515 (1979)
19. H.Ryufuku and T.Watanabe, IAERI-memo 8337 (1979)
20. W.L.Nutt, R.W.McCullough, K.Brady, M.B.Shah and H.B.Gilbody, J.Phys.B 11, 1457 (1978)
21. K.H.Berkner, W.G.Graham, R.V.Pyle, A.S.Schlachter, J.W.Stearns and R.E.Olson, J.Phys.B 11, 875 (1978)
22. K.H.Berkner, W.G.Graham, R.V.Pyle, A.S.Schlachter, J.W.Stearns, Phys.Lett.62A, 407 (1977)
23. see for example: R.A.Mapleton, Theory of Charge Exchange (Wiley, New York, 1972)

24. H.Eubank et al., Phys.Rev.Lett.43, 270 (1979)
25. D.L.Jassby, Nucl.Fusion 17, 309 (1977)
26. J.D.Garcia, E.Gerjuoy and J.E.Welker, Phys.Rev.165, 66 (1968)
27. L.P.Presnyakov and A.D.Ulantsev, Sov.J.Quant.Electronics 4, 1320 (1975)
28. M.I.Chibisov, JETP Lett.24, 46 (1976)
29. T.P.Grozdanov and R.K.Janev, Phys.Rev.A17, 880 (1978)
30. E.Salzborn and A.Müller, Proc.XI.Intern.Conf.on the Physics of Electronic and Atomic Collisions, Kyoto (1979), (to be published)
31. H.Klinger, A.Müller and E.Salzborn, J.Phys.B 8, 230 (1975)
32. A.Müller, H.Klinger and E.Salzborn, Phys.Lett.55A, 11 (1975)
33. E.Salzborn, Proc.Intern.Conf.on Heavy Ion Sources, Gatlinburg (1975), IEEE Trans.NS-23, 947 (1976)
34. A.Müller and E.Salzborn, Phys.Lett.59A, 19 (1976)
35. H.Klinger, A.Müller and E.Salzborn, J.Chem.Phys.65, 3427 (1976)
36. A.Müller and E.Salzborn, Phys.Lett.62A, 391 (1977)
37. A.Müller, Ch.Achenbach and E.Salzborn, Phys.Lett.70A, 410 (1979)
38. R.E.Olson, Phys.Rev.A18, 2464 (1978)
39. A.Salop, J.Phys.B 12, 919 (1979)
40. J.A.Guffey, L.D.Ellsworth and J.R.MacDonald, Phys.Rev. A15, 1863 (1977)
41. H.Winter, E.Bloemen and F.J.de Heer, J.Phys.B 10, L 311, L 454, L 599 (1977)
42. A.Niehaus and M.W.Ruf, J.Phys.B 9, 1401 (1976)
43. P.H.Woerlee, T.M.El Sherbini, F.J.de Heer and F.W.Saris, J.Phys.B 12, L 235 (1979)
44. V.V.Afrosimov, A.A.Basalaev, G.A.Leiko and M.N.Panov, Sov.Phys.JETP 47, 837 (1978)
45. H.F.Beyer, R.Mann, F.Folkmann and K.-H.Schartner, Proc.XI. Intern.Conf.on the Physics of Electronic and Atomic Collisions, Kyoto (1979), Book of Abstracts, p.602, 604
46. R.C.Isler, Phys.Rev.Lett.38, 1359 (1977)
47. R.C.Isler and E.C.Crume, Phys.Rev.Lett.41, 1296 (1978)
48. E.D.Donets, IEEE Trans.Nucl.Sci.NS-23, 897 (1976)
49. J.Arianer and Ch.Goldstein, Institut de Physique Nucleaire, Orsay, Report IPNO-79-02

ELECTRON-ION COLLISIONS: EXPERIMENTAL

Gordon H. Dunn*

Joint Institute for Laboratory Astrophysics
National Bureau of Standards and University of Colorado
Boulder, Colorado 80309 U.S.A.

Electron-ion collisions have long been of interest because of the application to non-local thermodynamic equilibrium modeling of astrophysical phenomena. Significant further impetus has arisen in the past several years as the understanding of such collisions has been recognized as necessary in the development of controlled thermonuclear fusion. Despite the long interest and the importance, the experimental study of these processes is recent. In 1961 Dolder et al.[1] published their measurement of electron-He^+ ionization, and since that time about 100 papers have appeared on electron-ion ionization and excitation cross sections and rates. Seaton[2] has recently reviewed the field with primary emphasis on the theory. Dolder and Peart[3] have written an excellent review covering the experimental cross-section work through about 1975. The bibliographies in those reviews as well as several other bibliographies[4-6] serve as good guides to the primary literature.

The purpose of this brief paper will not be to repeat or try to improve upon recent reviews,[2,3] but rather to look at work done since they were published and, where possible, to make unifying or speculative comments about the data. Because of the focus on very hot plasmas (fusion), attention will be limited to atomic ions; though there is a significant literature for electron-molecular ion collisions, especially for dissociative recombination.

We will consider excitation first, then ionization, and finally -- even more briefly -- dielectronic recombination.

EXCITATION

In Fig. 1 the filled-in squares represent ionic charge-atomic number species for which excitation cross section measurements have been made. Of course, such a simple plot cannot show the multiplicity of transitions for which measurements are possible on a single specie. We see only about 0.3% of the space filled in -- even for this incomplete plot; and there is only one isoelectronic sequence (Li-like ions) for which there is more than one measurement. A similar plot (not shown) for excitation rate measurements is similarly sparse (showing 20 entries rather than 14) but shows work on three isoelectronic sequences.

Clearly, one cannot and should not think it desirable or necessary to make measurements on all species, i.e., fill in the plot. Rather, the object of the limited number of possible measurements must be: 1) to increase physical understanding of the processes, e.g. by showing up unusual behavior or additional mechanisms not included in the theory; 2) to demonstrate the accuracy and adequacy of both sophisticated theory and simple "universal" formulae to predict cross sections for a process; and 3) to increase the data base for users. Ultimately, one must rely on theory and/or predictive formulae for

*Staff Member, Quantum Physics Division, National Bureau of Standards.

knowledge about most of the species now represented by the great white field in Fig. 1. In fact, of course, much theory and some predictive formulae do now exist to give much information, but their adequacy is not readily assessable because of the paucity of experimental data with which to compare. As noted earlier, theory for excitation of ions has been reviewed by Seaton[2] in 1976, and a new review by Henry[7] is in preparation.

All the known cross section measurements for electron-impact excitation of ions have been performed using the crossed beams technique, where a beam of electrons crosses a beam of ions, and fluorescence is observed in a third perpendicular direction. Measurables include beam currents, beam spatial distributions, absolute detector sensitivity (including spatial variation), and signal strength. Because target densities are low ($\sim 10^6$ cm^{-3}) and detection sensitivities are small ($\sim 10^{-4}$), signal rates can range from very small (e.g. 0.06 counts sec^{-1})[8] to moderate (e.g. 50 counts sec^{-1}).[9] With the presence of about 10 counts sec^{-1} background, in the measurement of the excitation of the 2^3P level of Li^+ this led to data times as long as 80 h for a single point with adequate statistical precision. More commonly, data times are of the order 1 to 2 hours per point. Absolute radiometry is usually, however, the most demanding task in the measurements. Despite the difficulties, much of the work has been pursued to give absolute cross sections accurate to better than 10%.

Li-like ions. Since the reviews cited,[2,3] work has been completed on measuring the cross sections for excitation of the 2^2P levels of three members of the Li-like isoelectronic sequence Be II,[10] C IV,[11] N V.[12] The effect of coupling of higher excited states is expected to diminish as Z is increased, since the 2S-2P separation varies as Z+1, while energies of higher n levels varies roughly as $(Z+1)^{1.8}$. Experimental results for C IV and N V were found to be in good agreement with theory, whereas in Be II the experimental cross sections are roughly 15% below theoretical values at all energies. There is also disagreement between measured and theoretical polarization of the emitted light in the Be II case.

He^+. The hydrogen-like structure is most attractive from the standpoint of comparing experiment and theory. Excitation of the 2s state was the first

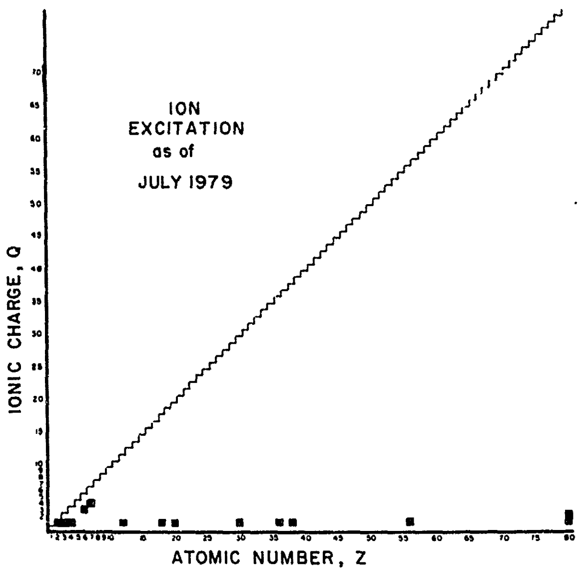

Fig. 1. Filled-in squares represent those species of charge Q and atomic number Z for which cross section measurements for excitation have been made.

measurement on excitation of an atomic ion. There has since been another high quality experiment that agreed with the first. In each case, the measurements were not absolute, and the cross section was normalized to high energy calculations corrected for cascade. This leads to a disagreement at low energies by a factor of 1.8 -- i.e., near threshold theory is 1.8 times greater than experiment. After 14 years this remains one of the greatest puzzles in electron-ion work. See Refs. 2 and 3 for further discussion and original references.

$\underline{Li^+}$. This He-like structure is the only member of the sequence on which measurements have been made.[8] The cross section was determined for excitation of the 2^3P level, and represents the only measurement of excitation of an ion from a singlet to a triplet level. A variety of theoretical approaches have yielded results that vary by more than a factor of two, and none appears to agree with the experimental cross sections really well (~50% disagreements). From only a few eV above threshold, the $1/E^3$ energy dependence seems to be in evidence.

Alkali structures.[2,3] In addition to the Li-like ions mentioned above (Be II, C IV, N V), ions of alkaline earths -- Mg II, Ca II, Sr II, Ba II -- have alkaline-like structures corresponding to Na, K, Rb, Cs, respectively. Excitation of the resonance levels and some of the cascading levels for all four species have been studied. For Ca II there has been extensive theoretical work because of the astrophysical interest. Comparison with three-state close coupling calculations of Burke and Moores at low energies shows theory high by about 35%. Results at high energies for Ca II and Ba II agree with Coulomb-distorted wave calculations. For Mg II, agreement between experiment and close coupling calculations seems better (in magnitude, not shape) than for Ca II, but the experimental result probably has a double size contribution from the 3d-3p transition, which is the same (within instrumental resolution) wavelength as the resonance line and also cascades into the resonance level. Thus, it is difficult to assess the significance of this approximate agreement.

Other ions.[2,3] Other ions studied include Ar II, Kr II, Zn II and Hg II, III. For the Ar II, Kr II transitions there are no theoretical results. For Hg II there is reasonable agreement at high energy with the simple Gaunt factor predictor formula. Neither experimental[13] nor theoretical[14] results for Zn II are yet published, but experiment and close coupling theory are in disagreement ranging around 30%.

It is instructive to consider the extent to which universal predictor formulas are effective. The most widely used such formula is the effective Gaunt factor formula[2] for resonance levels, which gives the cross section in units πa_0^2 as

$$\sigma = \frac{8\pi}{\sqrt{3}} \frac{f}{(\Delta)^2} \frac{1}{\chi} \bar{g} \quad . \tag{1}$$

Here Δ is the threshold energy in Rydbergs, f is the oscillator strength of the transition, χ is the incoming electron energy in units of threshold energy, and $\bar{g}$ is the effective Gaunt factor. For the formula to be a general predictor formula, $\bar{g}$ should be a "universal" function of energy. The extent to which this is true for a few of the ions for which data are available is shown in Fig. 2.

Generally, we may conclude that for singly charged ions, theory has not yet accurately predicted cross sections. For multiply charged Li-like ions,

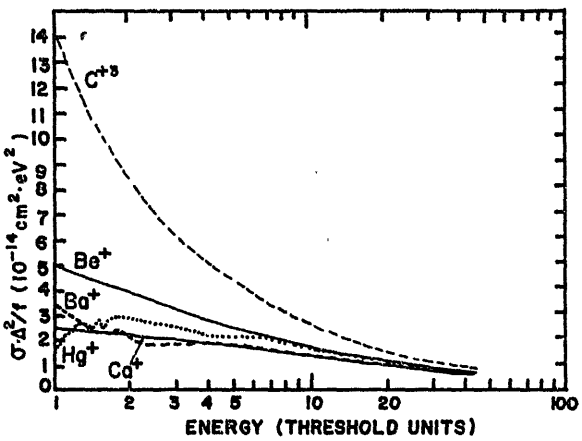

Fig. 2. Excitation cross section times square of threshold energy divided by oscillator strength versus electron energy in threshold units for the resonance lines of various ions as shown. Tests existence of a "universal" $\bar{g}$ curve.

theory and experiment agree well. The Gaunt factor predictor formula seems accurate to within the advertised factor of 2 for the singly charged ions measured, but does not work well for multiply charged ions for transitions with $\Delta n = 0$. More experiments need to be done on multiply charged ions along different isoelectronic sequences as well as on singly charged ions -- the "anchor" points.

IONIZATION

Figure 3, for ionization, is analogous to Fig. 1. Here the solid filled squares represent cross sections measured absolutely using crossed beams. The half shaded squares represent absolute measurements using trap methods, and the squares with dots in the center represent purely relative measurements using trap methods. The corresponding figure for rate measurements is even more sparse, having only 22 entries.

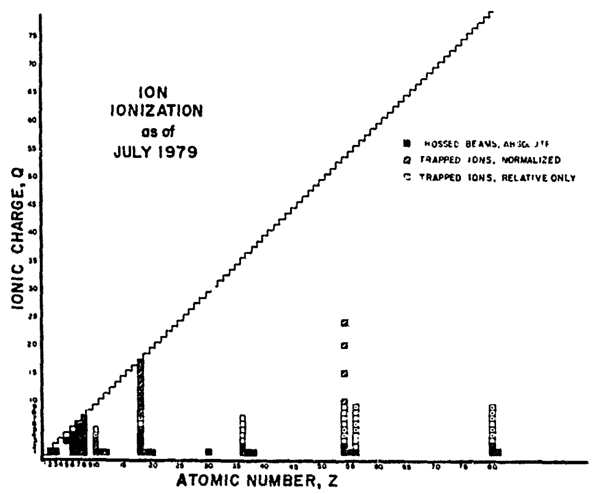

Fig. 3. Filled-in squares represent those species of charge Q and atomic number Z for which cross section measurements for ionization have been made. Point distinction is noted on plot.

Ionization proceeds through a variety of mechanisms

$$X^{+n} + e \rightarrow X^{+(n+1)} + 2e \qquad (2)$$

$$X^{+n} + e \rightarrow X^{+(n+1)*} + 2e \qquad (3)$$
$$X^{+(n+m)} + me$$

$$X^{+n} + e \rightarrow X^{+n*} + e \qquad (4)$$
$$X^{+(n+m)} + me \quad .$$

The process in Eq. (2) is direct knock-on ionization which can be visualized simply as a projectile electron imparting enough momentum to an outer shell electron to allow it to escape the field of the ion. The process in Eq. (3) involves, among other possibilities, the knock out of inner shell electrons with subsequent possible Auger ejection of other electrons to result in multiple ionization. The process in Eq. (4), referred to as excitation-autoionization involves excitation of an inner shell electron to a discrete state above the ionization continuum, followed by autoionization.

The number and complexity of the mechanisms involved, as well as the many-body nature of ionization have led to less rapid progress in the theory of ionization compared to excitation. Some work is being done in this area, however; for example, Moores[15] has developed Coulomb-Born codes for calculations with this method. Usually those needing ionization data have relied on semiempirical formulas[16] and scaling methods. Experiments are badly needed to test these. Experiments are (despite pitfalls and difficulties outlined by Dolder and Peart) generally easier for ionization than for excitation. This is primarily because the efficiency for detecting events is about 10^4 times greater, and absolute radiometry is not necessary.

Up through Dolder and Peart's 1976 review,[3] the only multi-charged species for which cross sections had been measured in beams were Mg III, N III, and O III, though a number of trap measurements had been made. Since that time, work on He-like ions B IV, C V, N VI; Li-like ions C IV, N V, O VI; Be-like ions N IV, O V; and O II and A V at Oak Ridge National Laboratory,[17-19] on Ar II, III, IV, V, VI at Giessen University,[20,21] and on Zn II at JILA[22] has nearly doubled the number of species for which we have absolute cross sections obtained by crossed beam measurements.

<u>He-like ions.</u>[17] The measurements on B IV, C V, and N VI were extremely difficult due to the tiny cross sections. The measurements all agree within experimental uncertainty with the cross sections calculated using either the Lotz formula or scaled Coulomb-Born.

<u>Li-like ions.</u>[17-19] The measurements on C IV, N V, O VI were done with considerable accuracy and dramatically show the effect of excitation-autoionization noted in Eq. (4). Results and comparison with theory are shown in Fig. 4 for O VI. The magnitude of excitation-autoionization is substantially larger than calculated. Crandall <u>et al.</u> find for these three species that the excitation-autoionization contribution increases rapidly with initial ionic charge. When some account is taken of excitation-autoionization, agreement with both legitimate theory and scaled formulas is generally within about 25% for all three species.

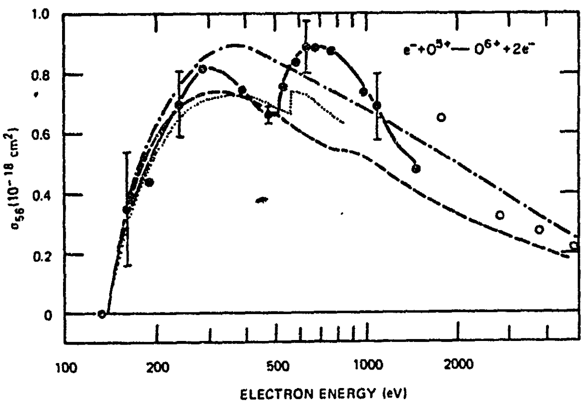

Fig. 4. Cross section for electron impact ionization of O VI. Closed points are Crandall et al.,[17,18] and are connected by a solid line. Open points are from Donets et al.[23]; dashed curve is scaled Coulomb-Born[24]; dot-dashed curve uses the Lotz formula[25]; and dotted curve is Coulomb-Born from Moores[26] including a contribution from excitation-autoionization calculated by R. J. Henry.

Be-like ions.[17] Work on N IV and O V is complicated by the presence of metastables in the beam, the fractional population of which may be as high as 50%. Assuming 50-50 mixtures of metastable and ground state ions, agreement is found with the Lotz formula, but not for scaled Coulomb-Born calculations.

Argon ions. In measurements of ionization of Ar^{n+} (n = 1-5) made by Müller et al.[20] the very remarkable result was found that all the results could be fit with a single formula

$$\sigma_{i,i+1} = \frac{1.4\times10^{-13}}{EI} \ell n\ (E/I)\ \mathrm{cm}^2 \qquad (5)$$

where E is electron energy and I the ionization energy in eV.

Müller and Frodl,[21] in another experiment, used crossed beams of electrons and multiply charged argon ions and looked at the resultant increase of charge state by more than one. Their results (an example is shown in Fig. 5) dramatically show that L-shell excitation followed by autoionization [Eq. (4)] strongly dominates multiple ionization.

Zn II.[22] This ion has a 4s electron followed by ten 3d electrons. Again, excitation-autoionization dominates over a part of the energy range (low energy). Surprisingly, the contribution of the ten 3d electrons is found to be substantially smaller than the simple single particle model and semiempirical Lotz formula predicts.

A systematic understanding of the relative importance of the different ionization mechanisms in Eqs. (2-4) needs to be developed for different electronic configurations. This implies substantial effort both experimentally and theoretically. It seems almost unbelievable that in many cases very simple scaling laws, empirical fitting formulas, etc., can predict ionization cross sections to fair accuracy. Yet, for some species the formulas seem to break down badly. Understanding when such breakdown can be expected, and for what reasons, is essential to the community of data users.

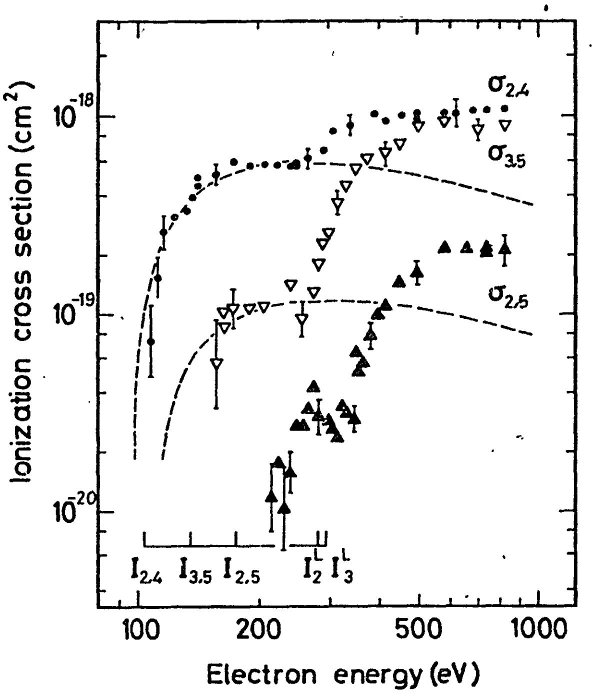

Fig. 5. Cross sections[21] for multiple ionization of Ar^{2+} and Ar^{3+} ions, broken lines are fitted cross sections for direct two-electron ionization; various ionization potentials I are indicated near the bottom.

DIELECTRONIC RECOMBINATION

An electron incident on an ion gains energy in the Coulomb field as the particles approach each other. Thus, an electron which at infinity has slightly less than the threshold energy for exciting an electron in the ion has more than enough by the time the two particles are together. If the projectile electron does excite the ion, then it is left with slightly less than enough energy to escape again to infinity. We thus have an ionic core excited electron and an electron in a high Rydberg state -- a doubly excited state which can autoionize. If the two excited electrons are weakly enough coupled, the core electron may radiate before autoionization occurs. The energy of the resultant Rydberg atom is then below the ionization continuum, a recombination has taken place -- so-called dielectronic recombination. As early as 1939 this process was hypothesized to be important in high temperature plasmas, and the evidence is now very strong that it is in many cases the dominant process. Seaton and Storey[27] have reviewed this process quite recently.

Despite the great importance and the interesting nature of the process, there have to date been no direct measurements of cross sections for this highly resonant process. A figure analogous to Figs. 1 and 3 would be entirely blank. There has been one paper on dielectronic recombination between electrons and K^+,[28] but the reference has not been accessible to this author. It is only in the past year that any rate measurements have been made, and it is interesting that two groups were able to simultaneously publish rate measurements, one[29] for Fe IX-XI, and one[30] for highly ionized (of the order of 30+) molybdenum ions. In both cases the plasma rate measurements were smaller than those calculated.

The problems associated with reliable and interpretable measurements stem from a variety of sources. The cross section will be highly resonant, and only electrons with very exactly defined energies will be effective. The Rydberg atoms resulting from a recombination are extremely fragile and subject to ionization by stray electric and magnetic fields and to re-ionization with very large cross sections in collision with electrons or gas. In addition, there are also the problems of small signals and high backgrounds present in excitation and ionization measurements. Despite the problems, a number of laboratories are working on these important measurements: Sheldon Datz at Oak Ridge; John Kohl at Harvard Smithsonian; Bill McGowan at Western Ontario; H. Suzuki at Sophia University and Nagoya; and others.

REFERENCES

1. K. T. Dolder, M. F. A. Harrison, and P. C. Thonemann, Proc. R. Soc. A 264, 367 (1961).
2. M. J. Seaton, in Advances in Atomic and Molecular Physics, Vol. 11, edited by D. R. Bates and B. Bederson (Academic, New York, 1975), pp. 83-142.
3. K. T. Dolder and B. Peart, Reports on Progress in Physics 39, 693 (1976).
4. L. J. Kieffer, Bibliography of Low Energy Electron and Photon Cross Section Data, NBS Special Publication 426, March 1976; E. C. Beaty and J. W. Gallagher, JILA Information Center Report No. 15, May 1976; ibid. Report No. 17, May 1977.
5. K. Takayanagi and T. Iwai, Bibliography on Electron Collisions with Atomic Positive Ions: 1940 through 1977, Report #IPPJ-AM-7, June 1978, Institute of Plasma Physics, Nagoya University, Nagoya, Japan.
6. There are two bulletins dealing with atomic data for fusion, the entire collection of either providing a substantial bibliography in electron-ion collisions: C. F. Barnett and W. L. Wiese, Atomic Data for Fusion, Oak Ridge National Laboratory, issued bimonthly. K. Katsonis et al., International Bulletin on Atomic and Molecular Data for Fusion, International Atomic Energy Agency, Vienna, issued quarterly.
7. R. J. Henry, private communciation, Aug. 1979.
8. W. T. Rogers, J. Ø. Olsen and G. H. Dunn, Phys. Rev. A 18, 1353 (1978).
9. P. O. Taylor and G. H. Dunn, Phys. Rev. A 8, 2304 (1973).
10. P. O. Taylor, R. A. Phaneuf and G. H. Dunn, private communication, 1979. To be published.
11. P. O. Taylor, D. Gregory, G. H. Dunn, R. A. Phaneuf and D. H. Crandall, Phys. Rev. Letters 39, 1256 (1977).
12. D. Gregory, G. H. Dunn, R. A. Phaneuf and D. H. Crandall, Phys. Rev. A 20, 410 (1979).
13. W. T. Rogers, G. Stefani, M. Reading, J. Ø. Olsen and G. H. Dunn, private communication, September 1979.
14. R. J. Henry, private communication, Sept. 1979.
15. D. L. Moores, J. Phys. B 11, 403 (1978).
16. For example, see the review: T. Kato, Ionization and Excitation of Ions by Electron Impact -- Review of Empirical Formulae, Report #IPPJ-AM-2, June 1977, Institute of Plasma Physics, Nagoya University, Nagoya, Japan.
17. D. H. Crandall, R. A. Phaneuf and D. C. Gregory, Electron Impact Ionization of Multicharged Ions, Report ORNL/TN-7020, September 1979, Oak Ridge National Laboratory.
18. D. H. Crandall, R. A. Phaneuf and P. O. Taylor, Phys. Rev. A 18, 1911 (1978).
19. D. H. Crandall, R. A. Phaneuf, B. E. Hasselquist and D. C. Gregory, J. Phys. B 12, L249 (1979).
20. A. Müller, E. Salzborn, R. Frodl, R. Becker and H. Klein, private communication, August 1979. Submitted to J. Phys. B.
21. A. Müller and R. Frodl, private communication, August 1979. Submitted to Phys. Rev. Letters.

22. W. T. Rogers, G. Stefani and G. H. Dunn, private communication, August 1979, to be submitted to Phys. Rev. A.
23. E. D. Donets and V. P. Ovsyannikov, Joint Institute of Nuclear Research, Dubna, Report No. P7-10780 (1977). (English translation ORNL-tr-4616 available from Technical Information Center, P. O. Box 62, Oak Ridge, Tenn. 37830).
24. L. B. Golden and D. H. Sampson, J. Phys. B 10, 2229 (1977).
25. W. Lotz, Z. Phys. 216, 241 (1968).
26. D. L. Moores, private communication, July 19, 1979.
27. M. J. Seaton and P. J. Storey, in Atomic Processes and Applications, edited by P. G. Burke and B. L. Moiseiwitsch (North Holland, Amsterdam, 1976), pp. 134-197.
28. I. S. Aleksakhin, A. I. Zapesochnyi and A. I. Imre, Pisma Zh. Ehksp. Teor. Fiz. 28, 576 (1978). In Russian.
29. R. L. Brooks, R. V. Datla and H. R. Griem, Phys. Rev. Letters 41, 107 (1978).
30. C. Breton, C. De Michelis, M. Finkenthal and M. Mattioli, Phys. Rev. Letters 41, 110 (1979).

PROGRAM

Nagoya Seminar on Atomic Processes in Fusion Plasmas

September 6-7, 1979

Institute of Plasma Physics, Nagoya University

September 6 (Thu)				
9:30	registration (coffee)			
10:00	Opening session: Chairman H. Suzuki			
	Welcome		K. Takayama	5 min
	Atomic processes in plasmas (a general review)		S. Hayakawa	35
	A & M data center activities			
		IAEA	K. Katsonis	30
		USA	E. C. Beaty	20
		GAPHYOR	A. Ricard J.L. Delcroix	10
		IPP	Y. Itikawa	10
12:00	lunch			
13:30	Session I: Chairman A. Dalgarno			
	Application of atomic collisions to the corpuscular diagnostics of high-temperature plasma (invited talk)		V.V. Afrosimov	30
	Plasma diagnostics on JIPP T-II Tokamak (invited talk)		J. Fujita	25
	Plasma diagnostics by neutral lithium beam probing		K. Kadota	5
	Density measurements of the excited atoms in plasma by means of optical fluorescence		K. Tsuchida	5
	Heavy ion beam probe for potential measurements		I. Katsumata Y. Sakai T. Oshio	5

	High di-electronic satellite lines in solar flare and fusion plasmas		
		J. Dubau M. Loulergue F.B. Dubau P. Faucher L.S. Clark A.H. Gabriel S. Volonte	5
15:30	coffee		
16:00	Special session: Chairman T. Sasaki		
	NICE project at IPP (invited talk)		
		Y. Kaneko	25
16:30	laboratory visit		
19:00	reception		
September 7	(Fri)		
9:00	Session II: Chairman K. Mori		
	Impurity radiation losses in fusion plasmas (invited talk)		
		D.E. Post	30
	Oxygen emission behavior of high density Tokamak plasma in JIPP T-II		
		K. Sato	5
	Spectroscopic observation of laser produced high density plasma	Y. Kato N. Miyanaga K. Mima	5
	Computer simulation on X-ray emission in laser plasma		
		K. Nishihara T. Yabe K. Mima N. Miyanaga Y. Kato	5
	Atomic potentials and transitions at high temperature and/or high density		
		R.H. Pratt Y.S. Kim I.J. Feng	5
10:30	coffee		
11:00	Session III: Chairman R.E. Olson		
	Atomic collisions in fusion plasmas involving multiply charged ions (invited talk)		
		E. Salzborn	30

Argon ion-argon atom charge changing collisions in the energy range 0.75 to 15 keV per incident charge

	S. Bliman N. Chantung R. Geller B. Jacquot D. van Houtte	5

Charge-transfer and impact-ionization cross sections for highly stripped carbon and niobium ions incident on argon and hydrogen

	A.S. Schlachter K.H. Berkner W.C. Graham R.V. Pyle J.W. Stearns	5

Low energetic charge transfer collisions of multiply charged ions

	B.A. Huber H.J. Kahlert H. Schrey K. Wiesemann	5

Charge transfer of multiply-charged ions at thermal energies

	A. Dalgarno	5

12:30 lunch

14:00 Session IV: Chairman Y.K. Kim

Electron-ion collisions: a review (invited talk)

	G.H. Dunn	30

Measurements of electron-ion collisions at Harvard-Smithsonian

	J.L. Kohl G.P. Lafyatis W.H. Parkinson	5

On the electron-ion collision experiment in progress in the IPP/Nagoya

	H. Suzuki K. Wakiya S. Ohtani A. Danjo	5

Electron-ion collisions in hot plasma

	Y. Hahn	5

Electron-ion collision processes involving H_2^+ and H_3^+

	J.Wm. McGowan W. Claeys P.M. Mul V.S. D'Angelo	5

15:30 concluding — J. Kistemaker

16:00 bus

Nagoya Seminar on Atomic Processes in Fusion Plasmas

Participants

Vadim V. Afrosimov
Ioffe Physical-Technical Institute
Academy of Sciences of the USSR
194021 Leningrad
USSR

Jacques A. Dubau
C.N.R.S.
Observatoire de Paris
92190-Meudon
France

Tsuneo Amano
Plasma Physics Laboratory
Faculty of Engineering
Osaka University
Yamada, Suitashi, Osaka 565
Japan

Gordon Harold Dunn
Joint Institute for Laboratory
Astrophysics
University of Colorado
Boulder, Colorado 80309
USA

Earl C. Beaty
Joint Institute for Laboratory
Astrophysics
University of Colorado
Boulder Colorado 80309
USA

I-Jaung Feng
Department of Physics
University of Pittsburgh
Pittsburgh, PA 15260
USA

Reinard Becker
Institut fuer Angewandte Physik
Robert-Mayerstrasse 2-4
D-6000 Frankfurt 1
FRG

Junji Fujita
Institute of Plasma Physics
Nagoya University
Furocho, Chikusaku, Nagoya 464
Japan

Samuel L. Bliman
Centre d'Etudes Nucléaires de Grenoble
85 X Avenue des Martyrs
38041 Grenoble, Cedex
France

J.-C. Gauthier
Institut d'Electronique Fondamentale
Bat 220, Universite Paris XI
91405 Orsay
France

Alexander Dalgarno
Center for Astrophysics
60 Garden Street, Cambridge
MA 02138
USA

Anna G. Giardini
Comitato Nazionale per l'Energia Nucleare
Centro di Frascati
CP 65, 00044 Frascati, Rome
Italy

Atsunori Danjo
Department of Physics
Niigata University
8050 Igarashi-ninomachi
Niigata 950-21
Japan

Y. Hahn
Physics Department
University of Connecticut
Storrs, Conn. 06268
USA

Hiroaki Hanashiro
Dept. of Pure & Applied Science
College of General Education
University of Tokyo
Komaba 3-8-1, Meguro-ku, Tokyo
Japan

Kiyoshi Kadota
Institute of Plasma Physics
Nagoya University
Furocho, Chikusaku, Nagoya 464
Japan

Satio Hayakawa
Institute of Plasma Physics
Nagoya University
Furocho, Chikusaku, Nagoya 464
Japan

Yozaburo Kaneko
Department of Physics
Tokyo Metropolitan University
Fukazawa 2-1-1, Setagayaku
Tokyo 158
Japan

Bernd A. Huber
Insitut für Experimentalphysik
Ruhr-Universität
4630 Bochum
FRG

Takako Kato
Institute of Plasma Physics
Nagoya University
Furocho, Chikusaku, Nagoya 464
Japan

P.N. Hvelplund
Institute of Physics
University of Aarhus
DK 8000 Aarhus C
Denmark

Yoshiaki Kato
Institute of Laser Engineering
Osaka University
Yamada, Suitashi, Osaka 565
Japan

R. Il'in
Ioffe Physico-Technical Institute
Academy of Sciences of the USSR
194021 Leningrad
USSR

Kosta Katsonis
International Atomic Energy Agency
P.O. Box 590
A-1011 Vienna
Austria

Yukikazu Itikawa
Institute of Plasma Physics
Nagoya University
Furocho, Chikusaku, Nagoya 464
Japan

Itsuo Katsumata
Research Institute for Atomic Energy
Osaka City University
Sugimotocho, Sumiyoshiku, Osaka 558
Japan

Tsuruji Iwai
Department of Physics
Osaka University
Machikaneyama 1-1, Toyonakashi
Japan

Satya P. Khare
Physics Department
Meerut University
Meerut-250001
India

Hee J. Kim
Oak Ridge National Laboratory
BLDG. 6003, P.O. Box X
Oak Ridge, TN 37830
USA

John L. Kohl
Harvard-Smithsonian Center for Astrophysics
60 Garden Street
Cambridge, MA 02138
USA

Yong-Ki Kim
Argonne National Laboratory
Argonne, Ill. 60439
USA

Toshio Kusakabe
Department of Reactor Engineering
Faculty of Science and Technology
Kinki University
Kowakae 3-4-1, Higashi-Osaka 577
Japan

Young Soon Kim
Department of Physics
University of Pittsburgh
Pittsburgh, Pa. 15260
USA

Steven T. Manson
Department of Physics
Georgia State University
Atlanta, Georgia 30303
USA

Masahiro Kimura
Faculty of Science
Osaka University
Machikaneyamacho, Toyonakashi 560
Japan

Atsushi Matsumoto
Department of Physics
Osaka University
Machikaneyamacho 1-1
Toyonakashi 560
Japan

Jacob Kistemaker
FOM-Institute for Atomic and Molecular Physics
Kruislaan 407
1098 SJ Amsterdam
The Netherlands

Takashi Matsuo
Department of Physics
Tokyo Metropolitan University
Fukazawa 2-1-1, Setagayaku
Tokyo 158
Japan

Marcel Klapisch
Racah Institute of Physics
Hebrew University
Jerusalem
Israel

Frederick H. Mies
National Bureau of Standards
B 268 Physics BLDG
Washington D.C. 20234
USA

Nobuo Kobayashi
Department of Physics
Tokyo Metropolitan University
Fukazawa 2-1-1, Setagaya
Tokyo 158
Japan

Kunioki Mima
Institute of Laser Engineering
Osaka University
Yamada, Suitashi, Osaka 565
Japan

Mikio Mimura
Research Institute for Atomic Energy
Osaka City University
Sugimotocho, Sumiyoshiku, Osaka 558
Japan

Nobuaki Noda
Institute of Plasma Physics
Nagoya University
Furocho, Chikusaku, Nagoya 464
Japan

Shoji Miyake
Welding Research Institute
Osaka University
Yamada, Suitashi, Osaka 565
Japan

Toshiatsu Oda
Faculty of Science
Hiroshima University
Higashisenda-machi, Hiroshima
Japan

Hiromu Momota
Institute of Plasma Physics
Nagoya University
Furocho, Chikusaku, Nagoya 464
Japan

Shunsuke Ohtani
Institute of Plasma Physics
Nagoya University
Furocho, Chikusaku, Nagoya 464
Japan

Kazuo Mori
Institute of Physical and
Chemical Research
Hirosawa, Wakoshi
Saitama 351
Japan

Kosuke Okamoto
ULVAC Corporation
Hagizono 2500, Chigasakishi
Kanagawa 253
Japan

Shinobu Nakazaki
Department of Applied Physics
Miyazaki University
Kirishima 1-1-1, Miyazaki
Japan

Kazuhiko Okuno
Department of Physics
Tokyo Metropolitan University
Fukazawa 2-1-1, Setagaya
Tokyo 158
Japan

Roy H. Neynaber
IRT Corporation
7650 Convoy Ct.
San Diego, California 92111
USA

Ronald E. Olson
SRI International
Molecular Physics Laboratory
Menlo Park, CA 94025
USA

Katsunobu Nishihara
Institute of Laser Engineering
Osaka University
Yamada, Suitashi, Osaka 565
Japan

M.N. Panov
Ioffe Physical-Technical Institute
Academy of Sciences of the USSR
194021 Leningrad
USSR

D.E. Post
Plasma Physics Laboratory
Princeton University
P.O. Box 451
Princeton, N.J. 08544
USA

Kuninori Sato
Institute of Plasma Physics
Nagoya University
Furocho, Chikusaku
Nagoya 464
Japan

R.H. Pratt
Department of Physics & Astronomy
University of Pittsburgh
Pittsburgh, Pennsylvania 15260
USA

Alfred S. Schlachter
Magnetic Fusion Energy Group
Lawrence Berkeley Laboratory
University of California
Berkeley, Calif. 94720
USA

A. Ricard
Plasma Physics Laboratory
Universite Paris-Sud
91405 Orsay
France

Anthony F. Starace
Behlen Laboratory of Physics
The University of Nebraska
Lincoln, Nebraska 68588
USA

Yoshiyuki Sakai
Research Institute for Atomic Energy
Osaka City University
Sugimotocho, Sumiyoshiku
Osaka 558
Japan

Hiroshi Suzuki
Department of Physics
Sophia University
Kioicho, Chiyodaku
Tokyo 102
Japan

E.G. Salzborn
Institut für Kernphysik
University of Giessen
Leihgesterner Weg 217
D-6300 Giessen
FRG

Hiroshi Takeuchi
Japan Atomic Energy Research Institute
Tokaimura, Nakagun
Ibaraki 319-11
Japan

H. E. Saraph
Dept. of Physics & Astronomy
University College London
Gower Street
London WC1 E6BT
United Kingdom

Keiji Tani
Japan Atomic Energy Research Institute
Tokaimura, Nakagun
Ibaraki 319-11
Japan

Taizo Sasaki
College of General Education
University of Tokyo
Komaba, Meguroku
Tokyo 153
Japan

Y. Terashima
Institute of Plasma Physics
Nagoya University
Furocho, Chikusaku
Nagoya 464
Japan

Michio Tomita
Department of Nuclear Engineering
Kyoto University
Yoshida-honmachi, Sakyoku
Kyoto
Japan

Kazuki Tsuchida
Institute of Plasma Physics
Nagoya University
Furocho, Chikusaku
Nagoya 464
Japan

Seiji Tsurubuchi
Department of Physics
Osaka University
Machikaneyamacho, Toyonaka 560
Japan

Sigeru Watanabe
Faculty of Education
Mie University
Kamihamacho, Tsushi
Japan

Milan Matić
Boris Kidric Institute of Nuclear Energy
P.O.B. 522, 11001 Beograd
Yugoslavia

Y.A. Vdovin
Moscow Engineering-Physics Institute
Kashirskoe Shosse 1
Moscow 115409
U.S.S.R.

Kazuo Takayama
Institute of Plasma Physics
Nagoya University
Furocho, Chikusaku
Nagoya 464
Japan

H. Winter
Institut für Allgemeine Physik
Technische Universität Wien
Karlsplatz 13, A-1040 Wien
Austria

Junichi Mizui
Institute of Plasma Physics
Nagoya University
Furocho, Chikusaku
Nagoya 464
Japan

Naohiro Yamaguchi
Institute of Plasma Physics
Nagoya University
Furocho, Chikusaku
Nagoya 464
Japan

B.M. Smirnov
Kurchatov Institute of Atomic Energy
Moscow 123182
U.S.S.R.